Squeeze Film Dampers
Operation, models and issues of interest

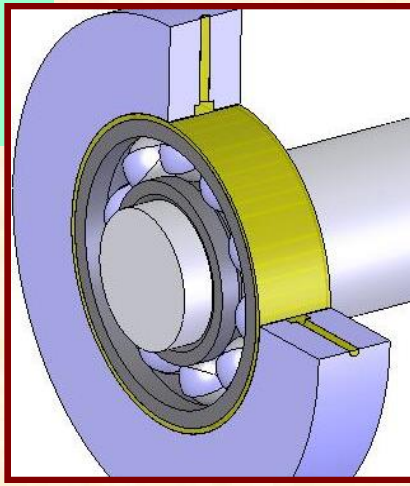

Luis San Andrés
Mast-Childs Chair Professor

J. MIKE WALKER '66 DEPARTMENT OF
MECHANICAL ENGINEERING
TEXAS A&M UNIVERSITY

Most common problems in rotordynamics

1. Excessive steady state synchronous vibration levels:

Improve balancing.

Modify rotor-bearing systems: tune system critical speeds out of RPM operating range.

SFDs

Introduce damping to limit peak amplitudes at critical speeds that must be traversed.

2. Subharmonic rotor instabilities

Eliminate instability mechanism, i.e. change bearing design if oil whip is present.

Rise natural frequency of rotor system as much as possible.

SFDs

Introduce damping to raise onset rotor speed above the operating speed range.

SFD Operation

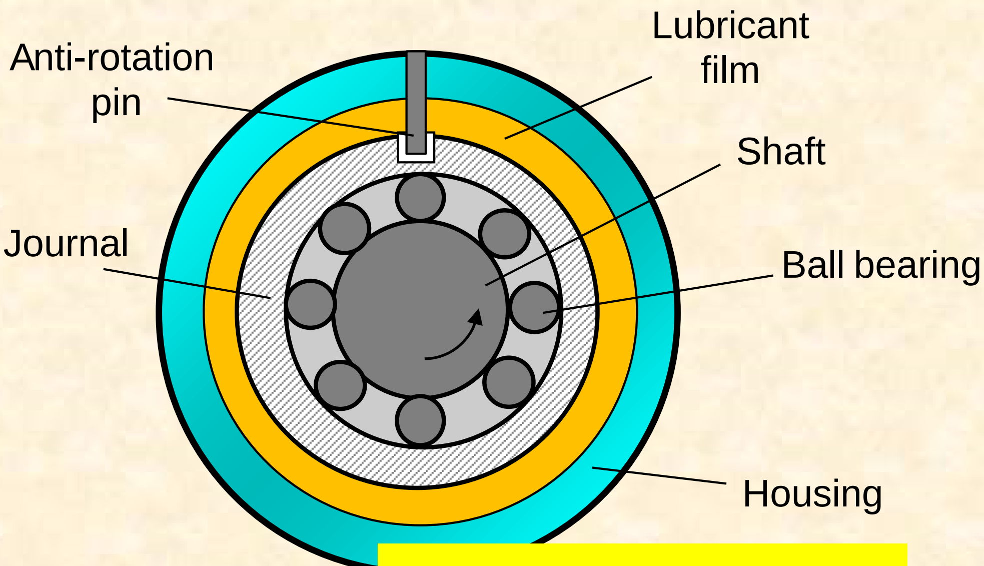

SFD with dowel pin

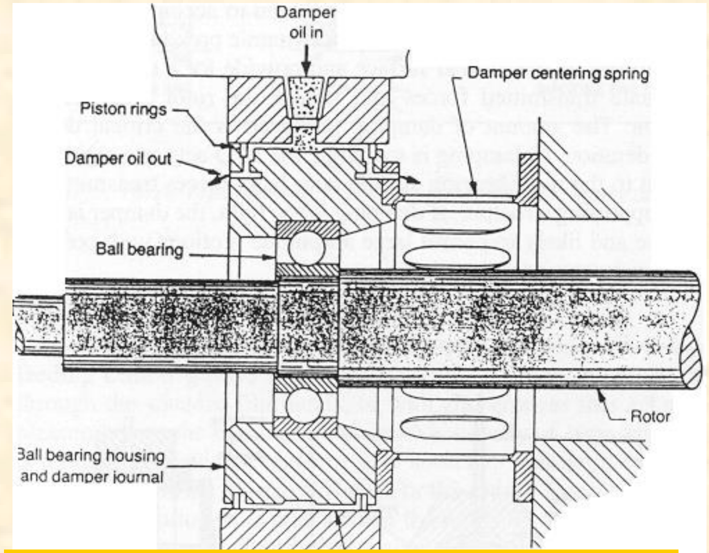

SFD with squirrel cage

Shaft mounted on ball bearings whose outer race cannot rotate (only whirl) with either a squirrel cage (US), or a dowel pin (UK).

In a SFD, the journal whirls but does not spin. The lubricant film is squeezed due to rotor motions, and fluid film (damping) forces are generated as a function of the journal velocity.

SFD dynamic forced performance

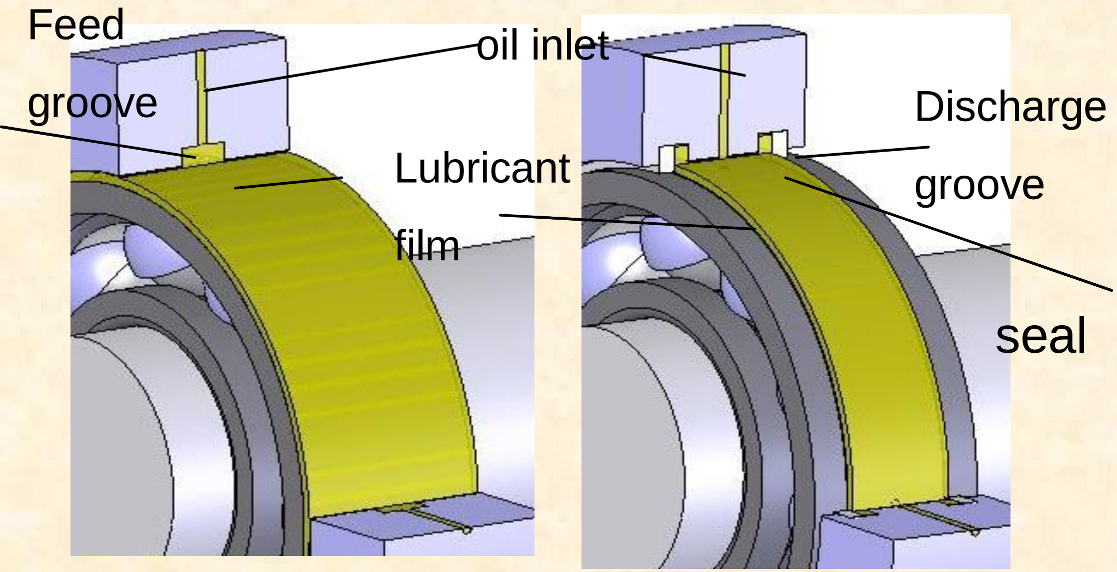

depends on

a) **Geometry** (*L*, *D*, *c*)

b) **Lubricant** (density, viscosity)

c) **Supply pressure and through flow conditions (grooves)**

d) **Sealing devices**

e) **Operating speed** (frequency) & **journal kinematics**

- **Flow regimes:** (laminar, superlaminar, turbulent)
- **Type of lubricant cavitation**:

  gaseous or vapor

  air ingestion & entrapment

Brief history of SFDs

Parsons (1889)

Discloses first use of a SFD as a part of the first modern-day steam turbine.

(by Topori at Polish Wikipedia)

Cooper (1963)

Rolls Royce engineer investigates experimentally the performance of rotating machinery with a SFD.

In 1970s, SFDs become essential components in aircraft engines and multistage high pressure centrifugal compressors.

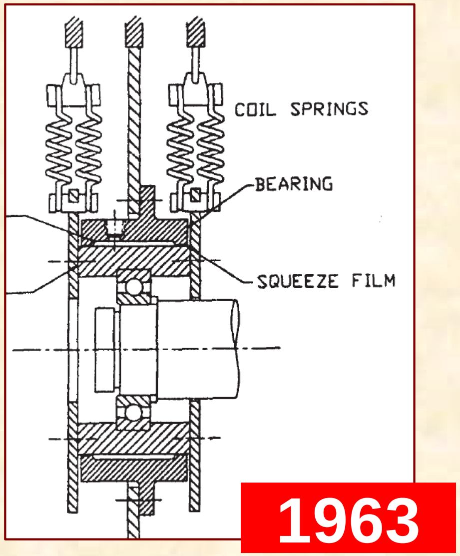

Brief history of SFD (Turbomachinery Symposium)

Zeidan et al. (1996)

History SFDs since 1960's and discuss major technical issues for their integration into turbomachinery, including oil cavitation vs. air ingestion and fluid inertia effects.

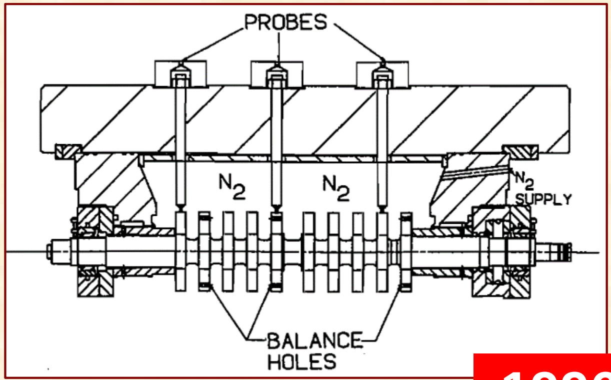

1996

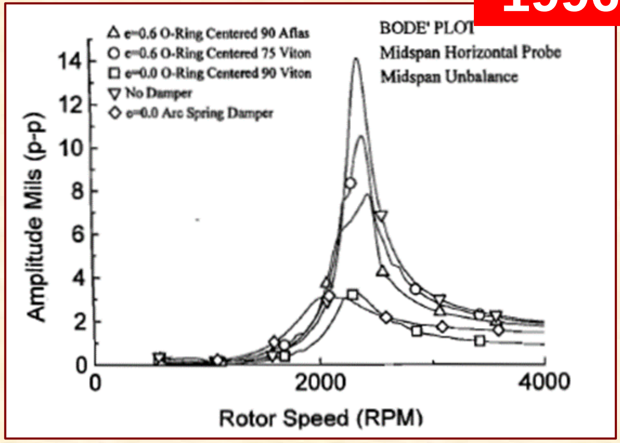

Kuzdal and Hustak (1996)

Tested various damper configurations (open and sealed ends) → optimized SFD reduces rotor synchronous motion amplitudes and raises stability threshold of a rotor bearing system.

Other relevant past work

- **Della Pietra and Adilleta (2002):** Comprehensive review of research conducted on SFDs over last 40 years.

Parameter identification in SFDs:

- **Tiwari et al. (2004):** Comprehensive review of parameter identification in fluid film bearings.

(2006-2010) San Andrés and Delgado (SFD & MECHANICAL SEAL, improved predictive models).

GT 2006-91238, GT 2007-24736, GT 2008-50528, GT 2009-50175

(2012-2021) San Andrés and students (sealed ends SFDs for aircraft)

GT 2012-68212 , GT 2013-94273 , GT 2014-26413, GT 20015-43096, GT 2016-43096, GT 2016-56695, 2016 A/TPS, GT2018-76224, GT 2019-90330, GT 2021-58627

SFD applications

Jet engines with rolling element bearings:

a) To reduce synchronous peak amplitudes,
b) Limit peak amplitudes at critical speeds,
c) To isolate structural components (lower transmissibility), and
d) To provide a margin of safety for blade loss.

Light hydrocarbon compressors with instability problems

a) To stabilize unit by introducing damping and reducing cross-coupled effect of seals, hydrodynamic bearings, etc.
b) To enhance limited damping available from tilting pad bearings.

Other benefits of SFDs on rotordynamic performance are:

- Tolerance to larger rotor motions * Simpler alignment
- Reduced balancing requirements * Less mount fatigue

Intershaft dampers

Multiple frequency excitation

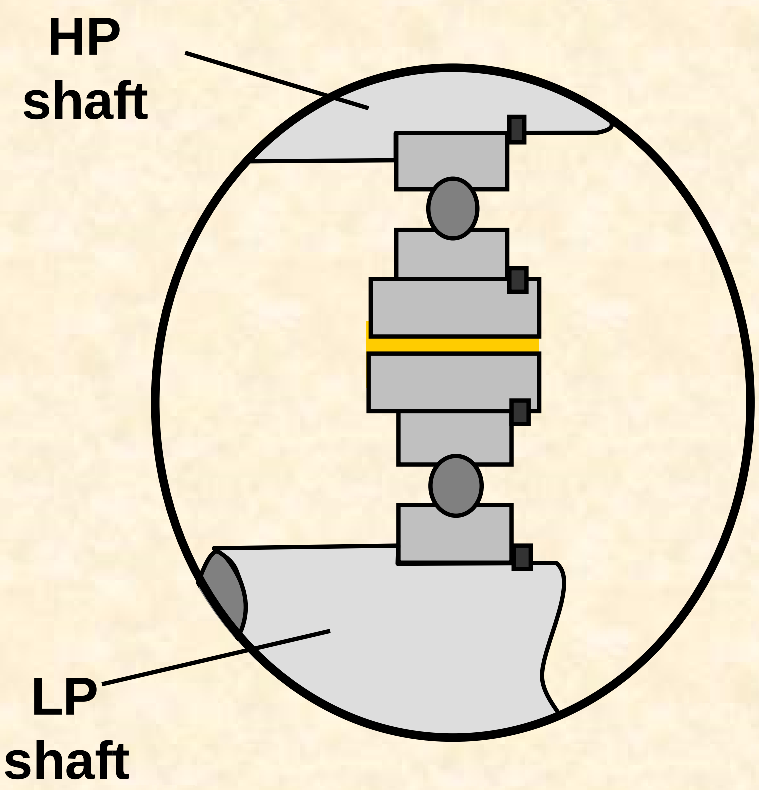

Schematic view of an intershaft SFD

In multi-spool jet engines, intershaft dampers locate at the interfaces between rotating shafts

Intershaft dampers whirl motions (precessional and spinning) result from the combined imbalance responses of both LP and HP rotors.

Types of end seals for SFDs

Reduce thru flow and increase damping.
Most seal types cannot prevent air ingestion

Industry uses O-rings, while jet engines use piston rings.

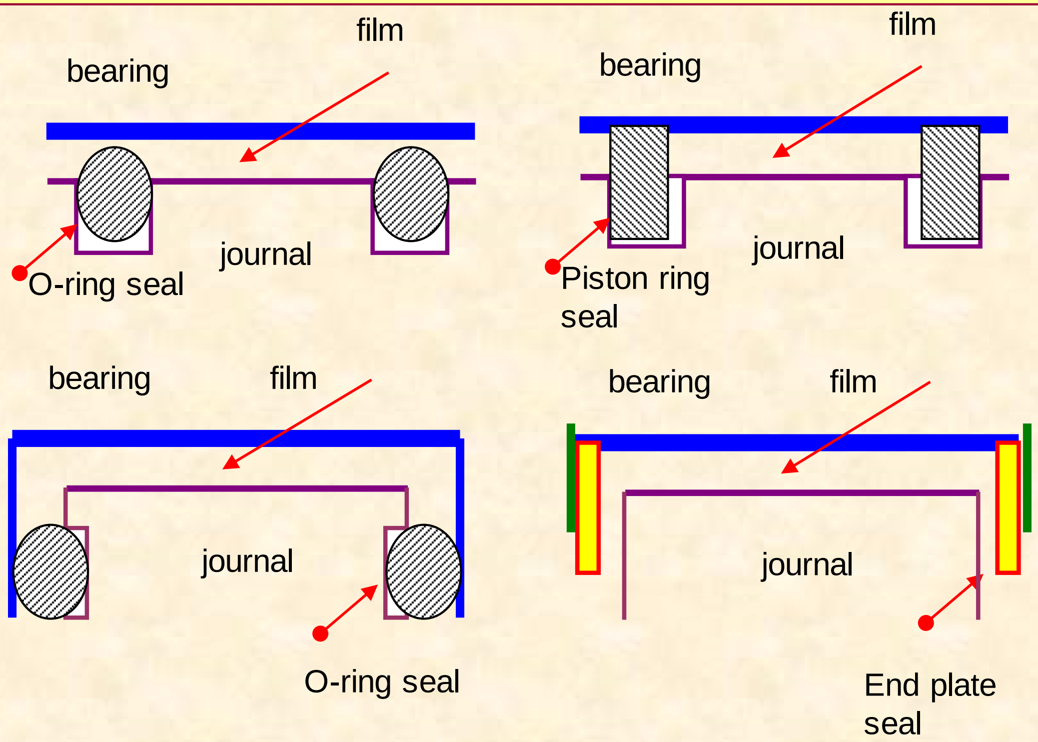

O-ring issues:

Low weight (replace squirrel cage),
Special groove machining,
Material compatibility

Piston ring issues:

Cocking and locking
Splits – leak too much

Design is highly empirical, except for end plate seals

SFD feed groove and exit grooves

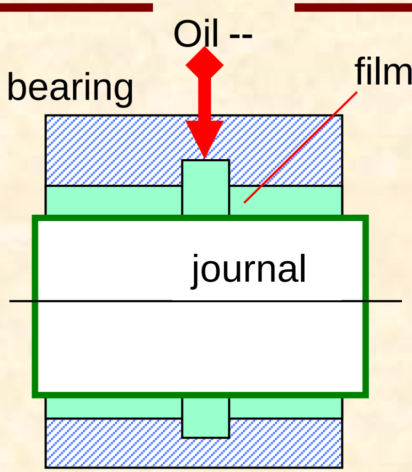

SFD with feed groove

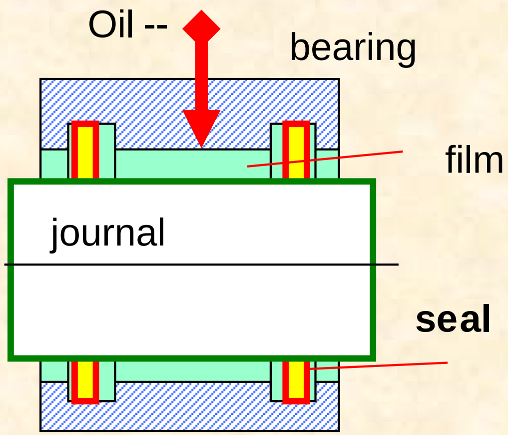

SFD with end grooves and seals

Feed holes with small diameter (high flow) resistance or with check valves prevent back flow and distortions in dynamic film pressures

Feed & discharge grooves

Interact with film flow, develop large dynamic film pressures, Induce inertia force coefficients even in small clearance (*c*) SFDs

Too shallow grooves: increase damping (d_g/c)<10

Too deep grooves: increase added mass (d_g/c)>10

Fundamental design consideration

The amount of damping (needed) is the critical design consideration.

If damping is too large the SFD acts as a rigid constraint to the rotor-bearing system with large forces transmitted to the supporting structure.

If damping is too low, the damper is ineffective and likely to permit large amplitude vibratory motion at synchronous and sub harmonic frequencies.

What is too large damping? What is too low?

What is the effect of viscous damping on the dynamic response of a mechanical system?

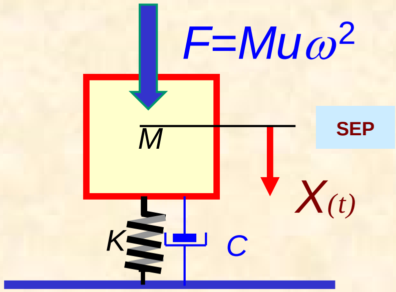

Simple spring-damper-mass system

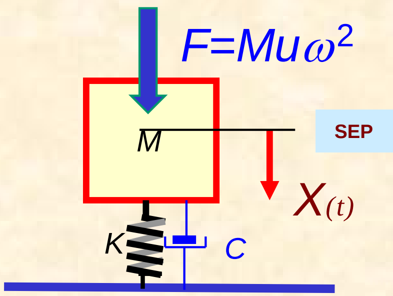

EOM: $M A_x = F - F_{damper} - F_{spring}$

$$M\ddot{X} + C\dot{X} + KX = F_{(t)}$$

System response defined by natural frequency (***f_n***) & damping ratio (ζ)

$$f_n = 2\pi\sqrt{K/M}\,;\ \zeta = C\big/2\sqrt{K\,M}$$

Response **amplitude** |***X/u***|

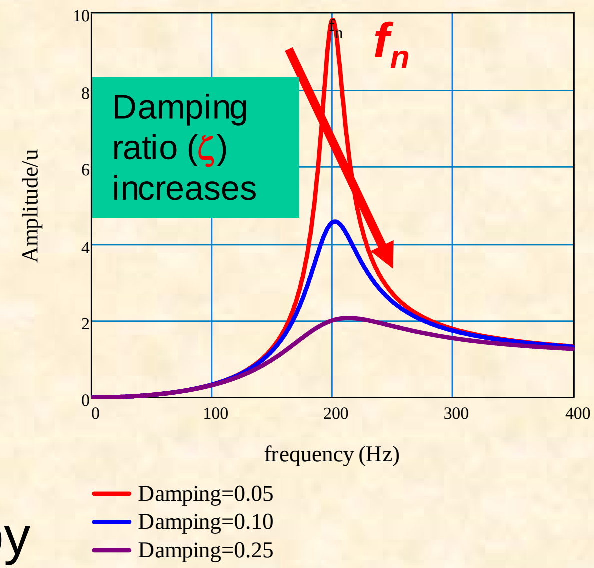

Transmissibility (to ground)

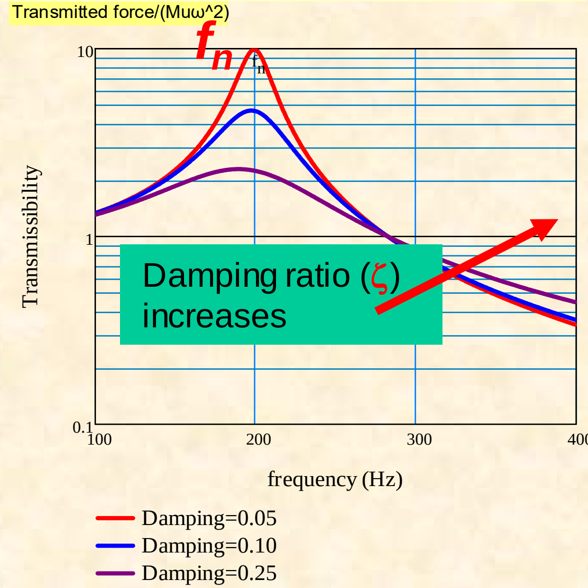

Damping helps only when rotor traverses a critical speed (natural frequency=***f_n***) but increases force transmissibility for operation above 1.44 ***f_n***

More complex K-C-M system : rotor on flexible supports

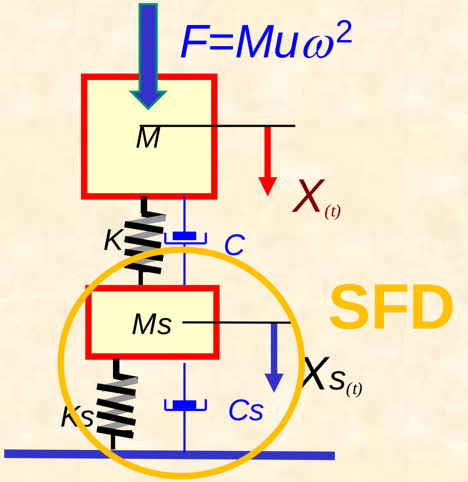

example

$$\frac{M_s}{M}=\frac{K_s}{K}=0.1;\ C=0;\ C_s \text{ varies}$$

Response amplitude |*X/u*|

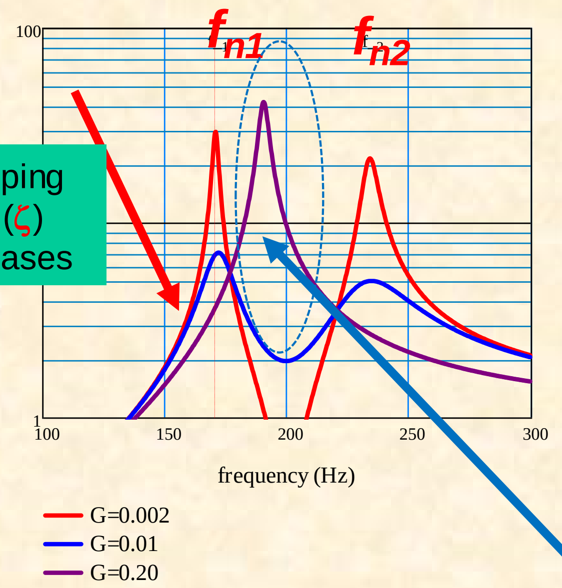

Damping ratio (ζ) increases

Transmissibility (to ground)

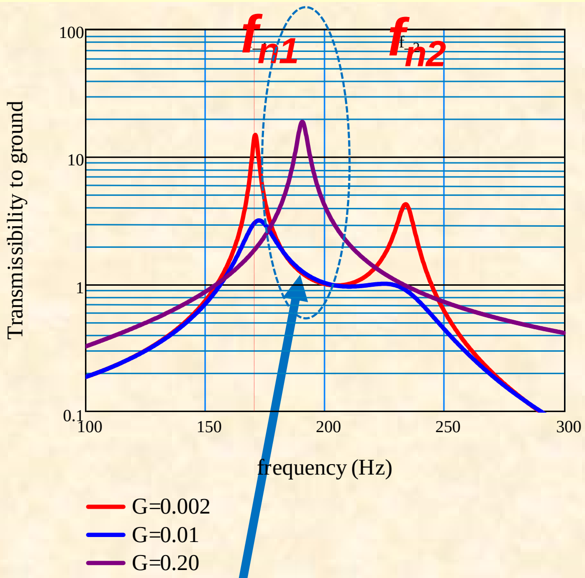

Excessive damping LOCKS supports and increases system response.

More complicated response. Damping helps only when traversing a critical speed (natural frequency=f_{n1} and f_{n2}) but increases force transmissibility.

SFDs – the bottom line

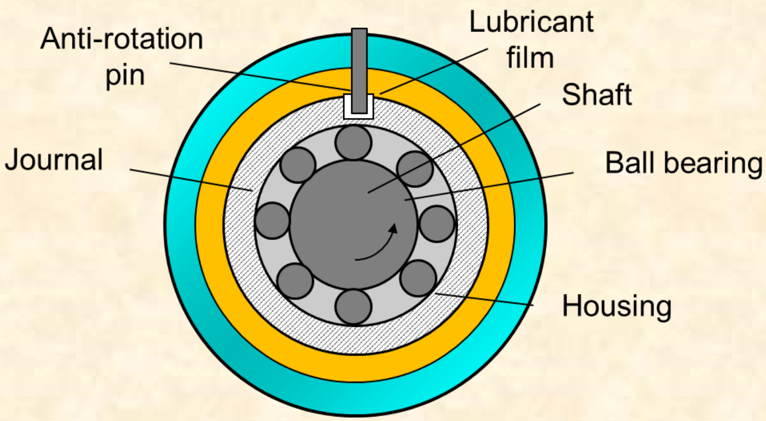

Too little damping may not be enough to reduce vibrations. **Too much damping** may lock damper & will degrade system performance.

SFDs must be designed with consideration of the whole rotor-bearing system.

Physical damping magnitude is not as important as the system damping ratio!

$$\zeta = C/C_{crit} = C/2\sqrt{K\,M}$$

SFD models for forced response

Damping is needed for safe passage through critical speeds and to provide or increase system stability.

Thus, models for SFD forced response are:

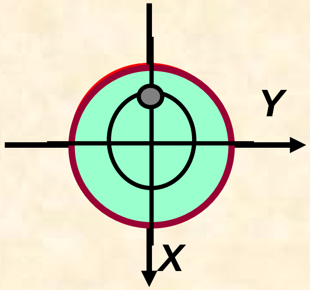

Imbalance response analysis:

SFD forces for circular centered whirl orbits.

Rotordynamic eigenvalue & stability analysis:

SFD force coefficients for dynamic journal motions about a static (equilibrium) position.

Numerical nonlinear formulations for transient response analysis of rotor-bearing response.

Abused in academic studies; nowadays too common with fast PCs

Journal bearing model: steady state

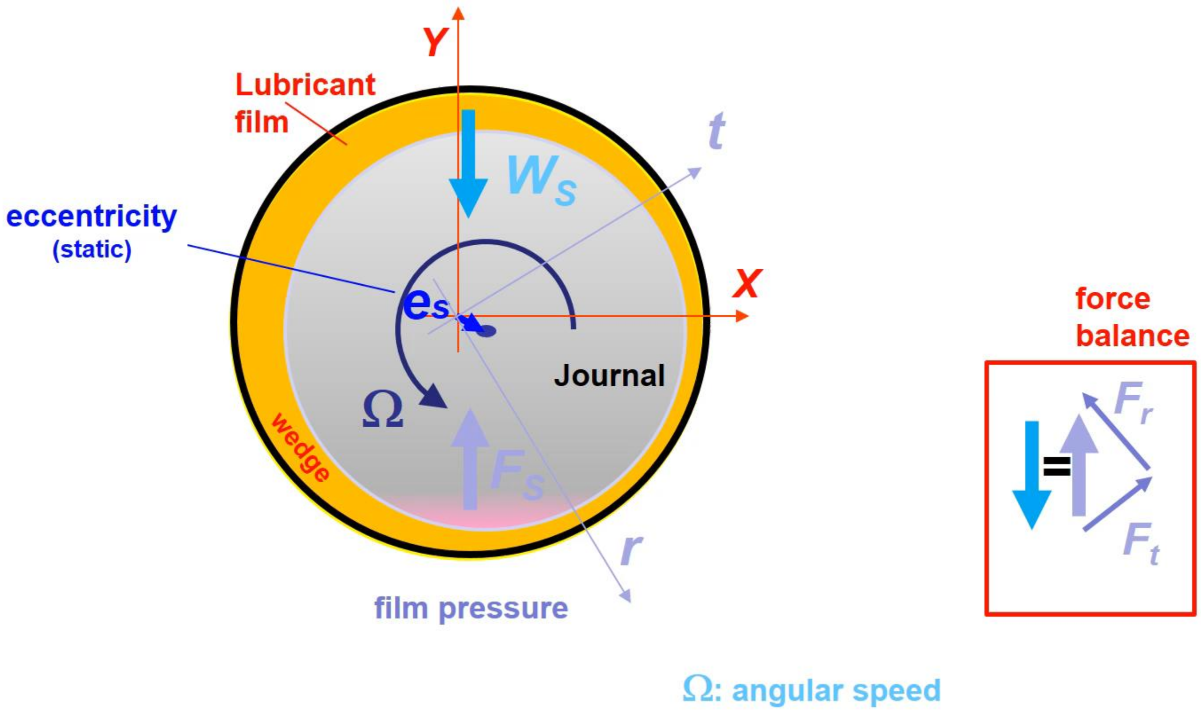

$v_t = 0$; $v_r=0$

$a_r = 0$; $a_t=0$

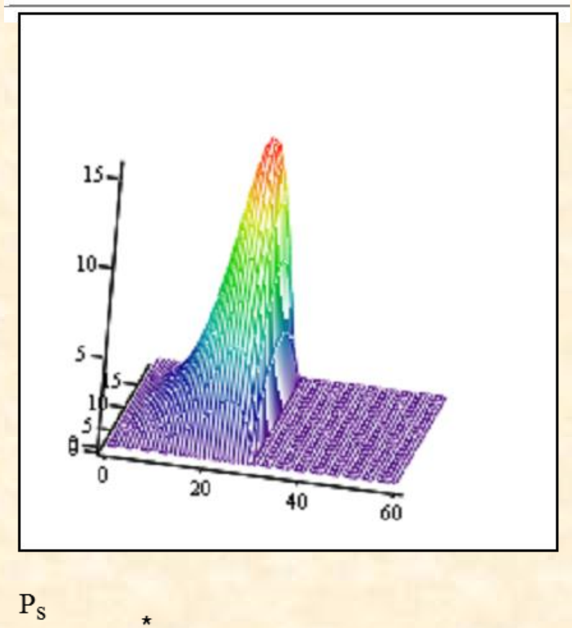

Pressure field is invariant with time and increases as film thickness decreases to a minimum.

SFD model: journal motions off-centered

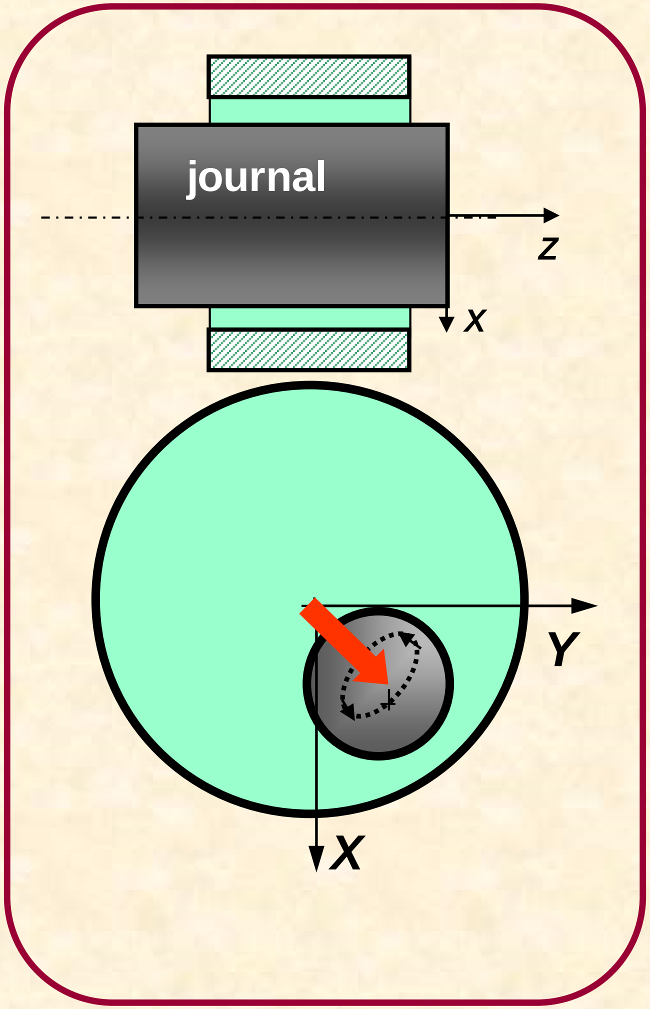

journal center displacements *(x,y)*

SFD reaction force for small amplitude motions about a static off centered journal position

$$-\begin{Bmatrix} F_X \\ F_Y \end{Bmatrix} = \begin{bmatrix} C_{XX} & C_{XY} \\ C_{YX} & C_{YY} \end{bmatrix} \begin{Bmatrix} \dot{x} \\ \dot{y} \end{Bmatrix} + \begin{bmatrix} M_{XX} & M_{XY} \\ M_{XY} & M_{YY} \end{bmatrix} \begin{Bmatrix} \ddot{x} \\ \ddot{y} \end{Bmatrix}$$

C: damping, **M:** inertia force coefficients

SFD force coefficients

NL functions of static journal eccentricity e_s

SFD model: pure radial squeeze (plunging motion)

0 ; $v_r = f(t)$

$a_r = 0$; $a_t=0$

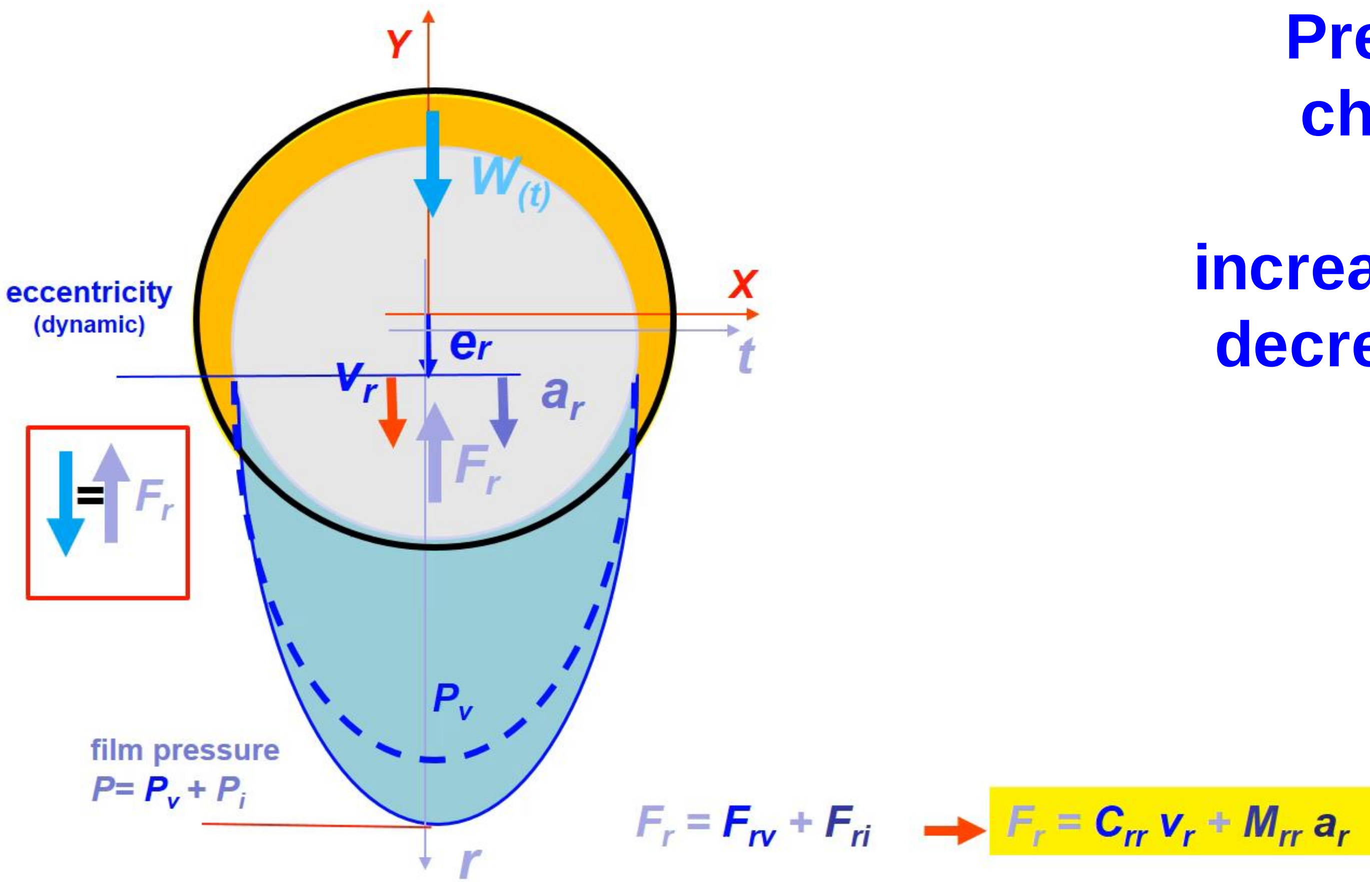

Pressure field changes with time and increases as film decreases. Note pressure reversals.

Kinetics of whirl (circular) orbits

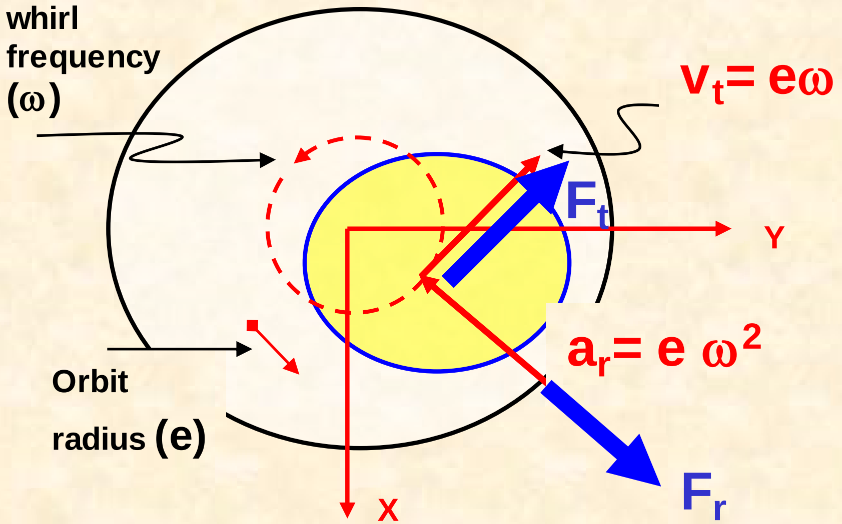

Journal center velocity with radial & tangential (v_r, v_t) components, and also acceleration (a_r, a_t)

For circular centered orbits, amplitude *e* is constant and whirl frequency = ω.

Circular centered orbit

$v_t = e\,\omega\;; \quad v_r = 0$

$a_r = -e\,\omega^2; \quad a_t = 0$

SFD reaction forces:

$$F_r = -(C_{rt}\, v_t + M_{rr}\, a_r)$$

$$F_t = -(C_{tt}\, v_t + M_{tr}\, a_r)$$

C: damping
M: inertia
coefficients

SFD model: circular centered orbits

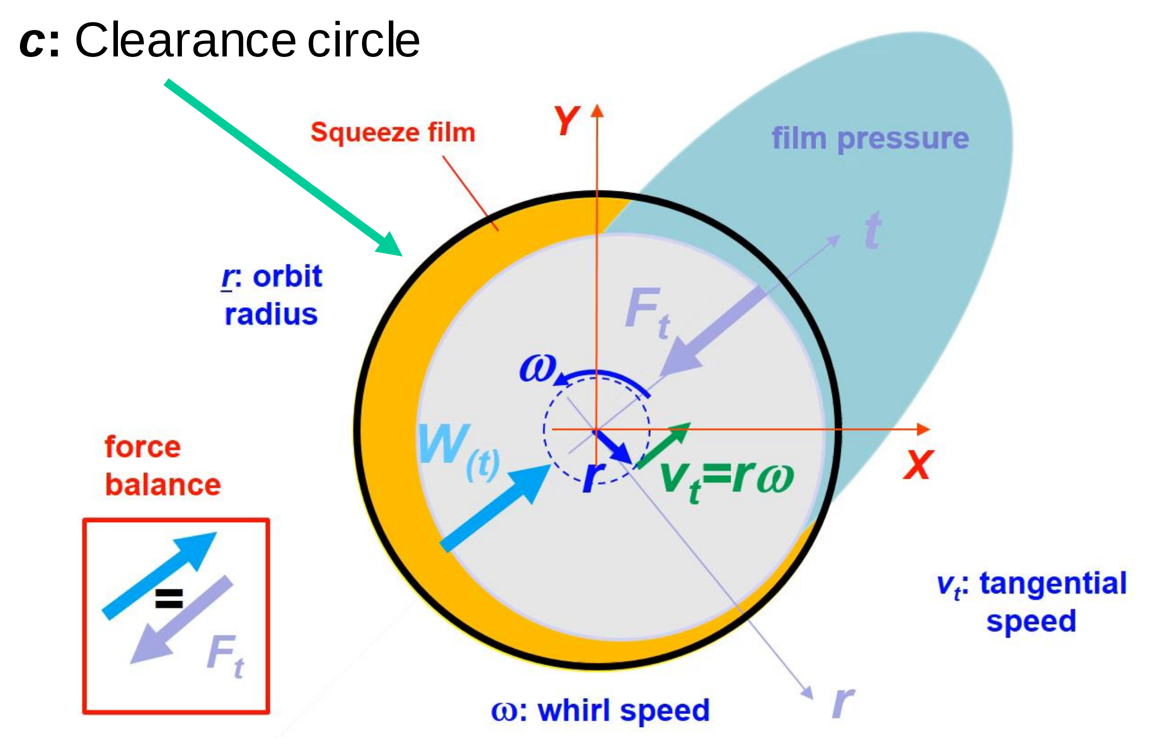

Circular centered orbit

$v_t = e\,\omega\,; \quad v_r=0$

$a_r = -e\,\omega^2; \quad a_t=0$

SFD reaction forces:

$$F_r = -(C_{rt}\, v_t + M_{rr}\, a_r)$$

$$F_t = -(C_{tt}\, v_t + M_{tr}\, a_r)$$

Pressure is invariant in rotating frame. *P* follows -d*h*/dt rather than *h* (film)

SFDs DO NOT have a stiffness

Misnomer: $K_{rr}=\omega C_{rt}$

SFD model: small amplitudes centered orbit

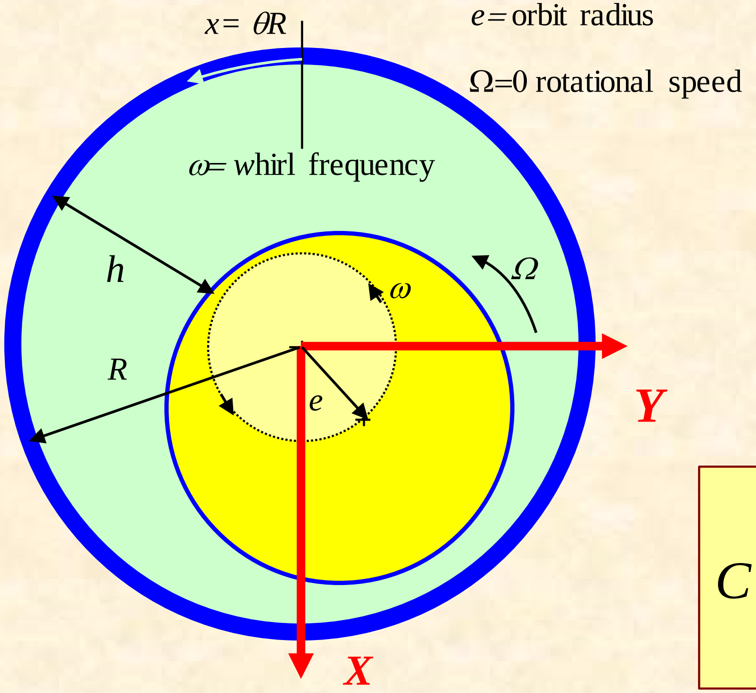

FULL FILM MODEL

Damping *(C)* & inertia *(M)* force coefficients by Reinhart & Lund (1975)

$$C_{XX}=C_{YY}=C_{tt}=12\pi\frac{\mu R^3 L}{c^3}\left[1-\frac{\tanh\left(L/D\right)}{\left(L/D\right)}\right]$$

$$M_{XX}=M_{YY}=M_{rr}=\pi\frac{\rho R^3 L}{c}\left[1-\frac{\tanh\left(L/D\right)}{\left(L/D\right)}\right]$$

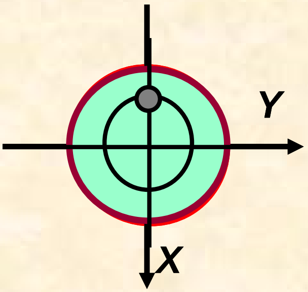

Damping ~ $(R/c)^3$, Inertia ~ R^3/c

SFD sealed vs open

FULL FILM MODEL

Open ends

$$C_{XX} = C_{YY} = C_{tt} = \tfrac{1}{2}\pi \frac{\mu D L^3}{c^3}$$

$$M_{XX} = M_{YY} = M_{rr} = \frac{\pi \rho D}{\mathbf{24}}\left(\frac{L^3}{c}\right)$$

(fully) Sealed ends

$$C_{XX} = C_{YY} = C_{tt} = \pi \frac{12}{8} \frac{\mu D^3 L}{c^3}$$

$$M_{XX} = M_{YY} = M_{rr} = \pi \frac{\rho D^3 L}{8c}$$

$$C_{tt} \frac{sealed}{open} = M_{rr} \frac{sealed}{open} = 3\left(\frac{D}{L}\right)^2$$

Increase in damping (and inertia) is large! For (L/D)=0.2=1/5, increase is **25x3** fold

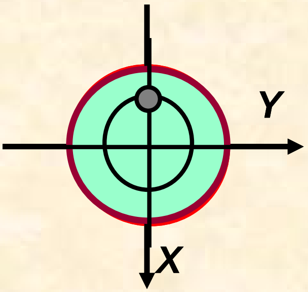

SFD model: circular centered orbits

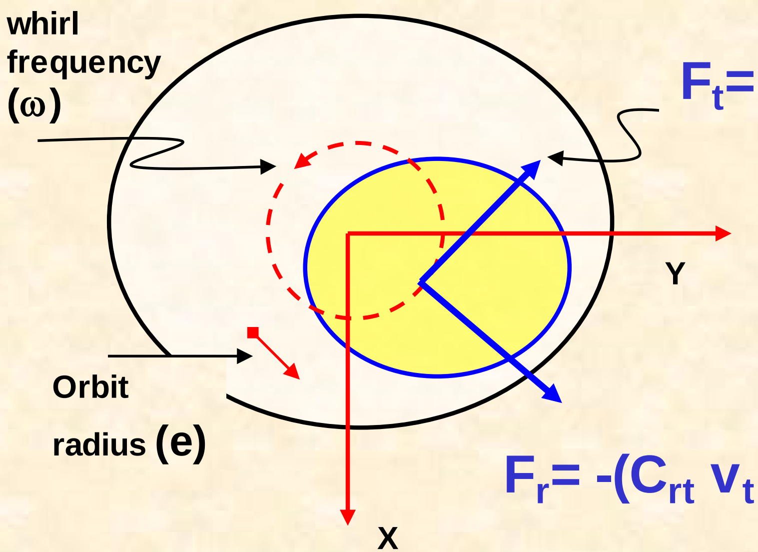

$F_t = -(C_{tt}\, v_t + M_{tr}\, a_r)$

$F_r = -(C_{rt}\, v_t + M_{rr}\, a_r)$

$v_t = e\,\omega$; $v_r = 0$
$a_r = -e\,\omega^2$; $a_t = 0$

π FILM MODEL

Damping & inertia force coefficients

Short length open ends SFD
(PI film model)

$$C_{tt} = \frac{\pi\,\mu\,D}{4\left(1-\varepsilon^2\right)^{3/2}}\left(\frac{L}{c}\right)^3; \quad C_{rt} = \frac{\mu\,\varepsilon\,D}{\left(1-\varepsilon^2\right)^2}\left(\frac{L}{c}\right)^3$$

$$M_{rr} = \frac{\pi\,\rho\,D}{24}\left(\frac{L^3}{c}\right)\left[1-2\left(1-\varepsilon^2\right)^{1/2}\right]\left\{\frac{\left(1-\varepsilon^2\right)^{1/2}-1}{\varepsilon^2\left(1-\varepsilon^2\right)^{1/2}}\right\};$$

$$M_{tr} = -\frac{27}{140\,\varepsilon}\,\rho\,D\left(\frac{L^3}{c}\right)\left[2+\frac{1}{\varepsilon}\ln\left(\frac{1-\varepsilon}{1+\varepsilon}\right)\right]$$

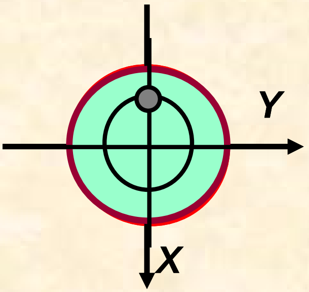

Damping ~ $(L/c)^3$, Inertia ~ L^3/c

SFD model: circular centered orbits

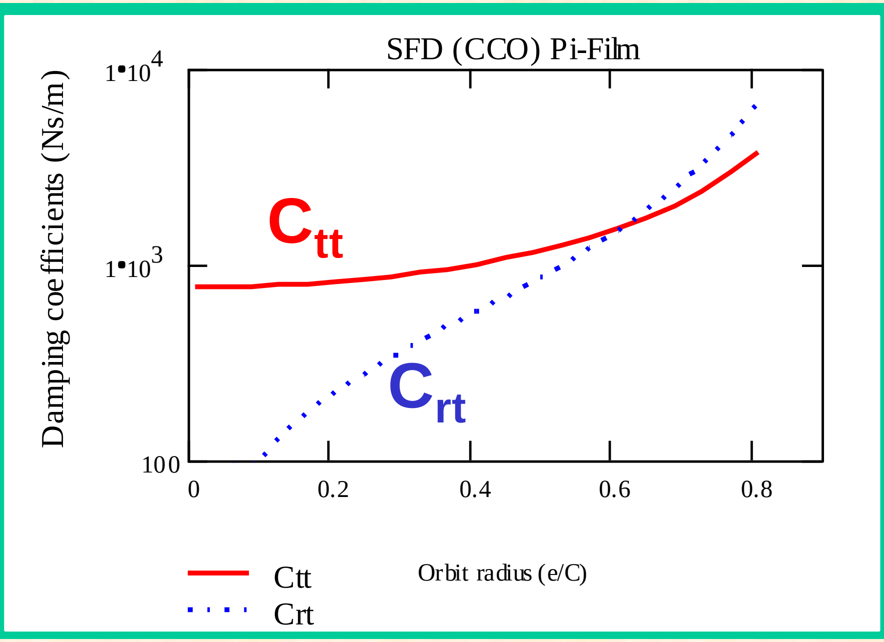

$L = 0.05$ m

$D = 0.2$ m

$C = 8 \cdot 10^{-4}$

$\mu = 0.02$ Pa.s

$\frac{L}{D} = 0.25$ $\frac{D}{C} = 250$

Short length open ends SFD π film model

$$F_r = -(C_{rt}\, v_t + M_{rr}\, a_r)$$

$$F_t = -(C_{tt}\, v_t + M_{tr}\, a_r)$$

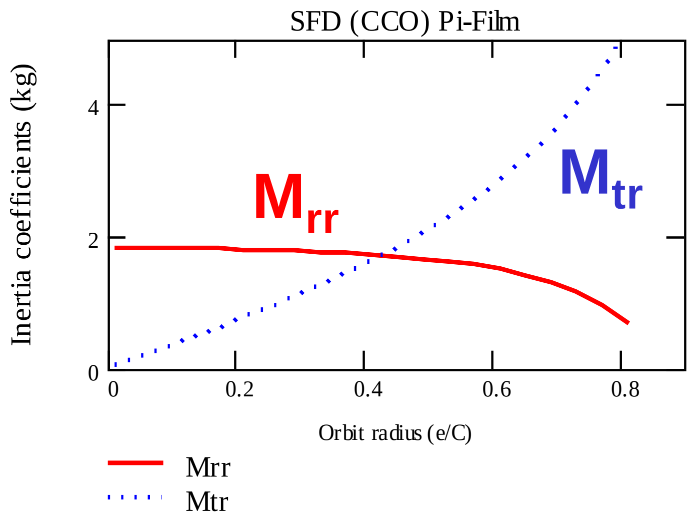

$M_j = 12.252$ kg - steel journal

$M_o = 0.022$ kg - lubricant

Nonlinear force coefficients,
Large damping,
Large inertia for
$Re_s = \rho\omega^2 c/\mu > 10$

Identification of SFD force coefficients for two SFDs: open ends & sealed ends

Sponsor: Pratt & Whitney Engines 2008-2018

SFD test rig

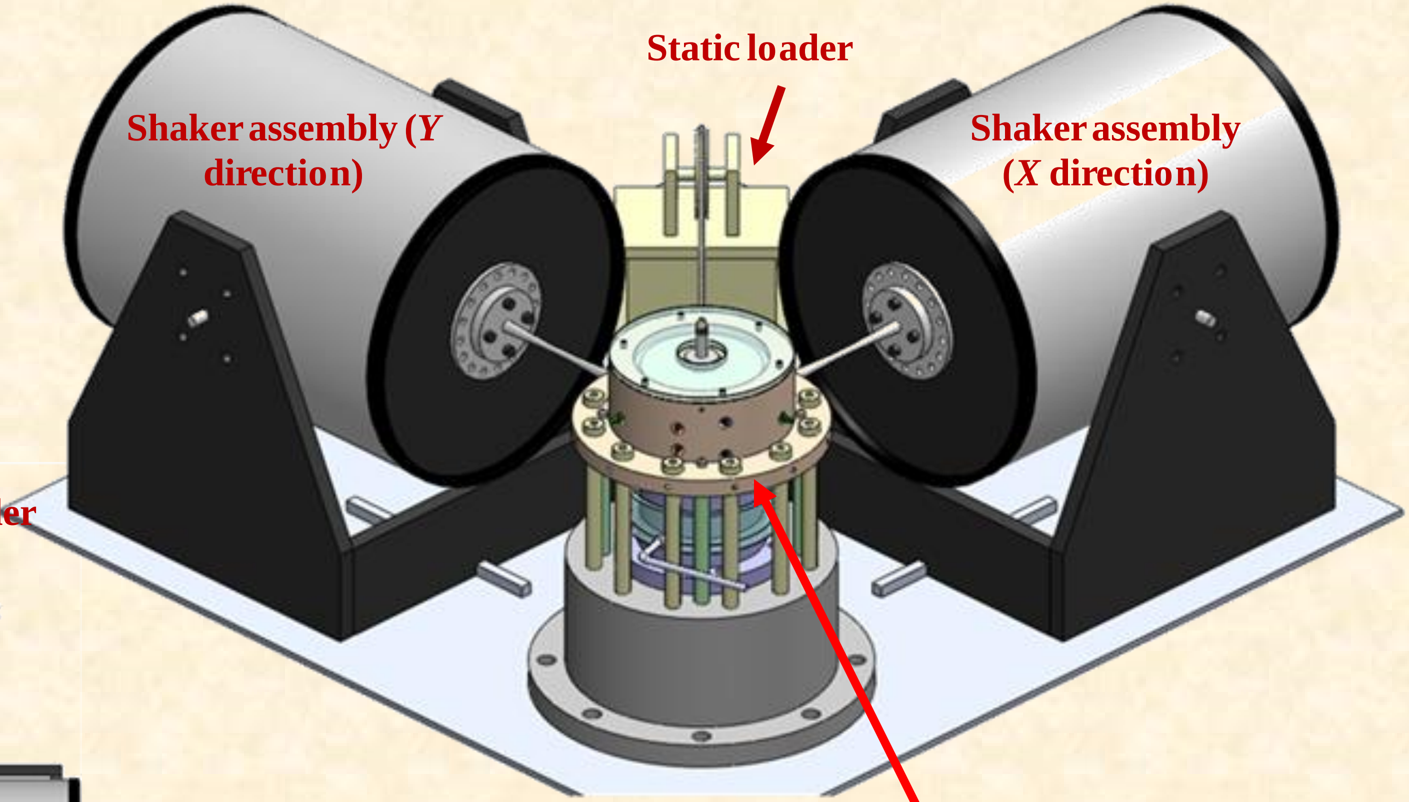

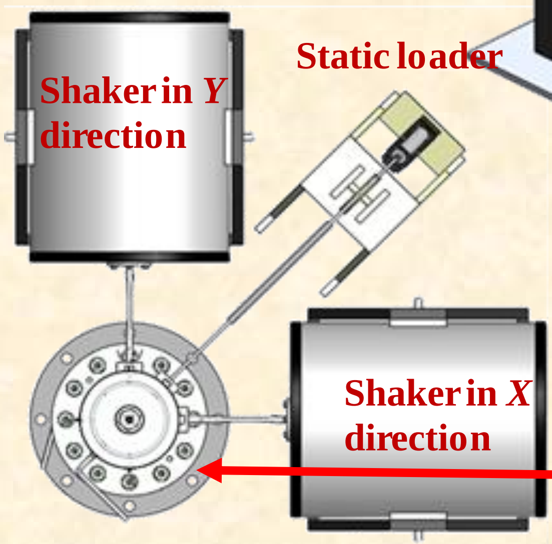

SFD test bearing

Test rig photograph

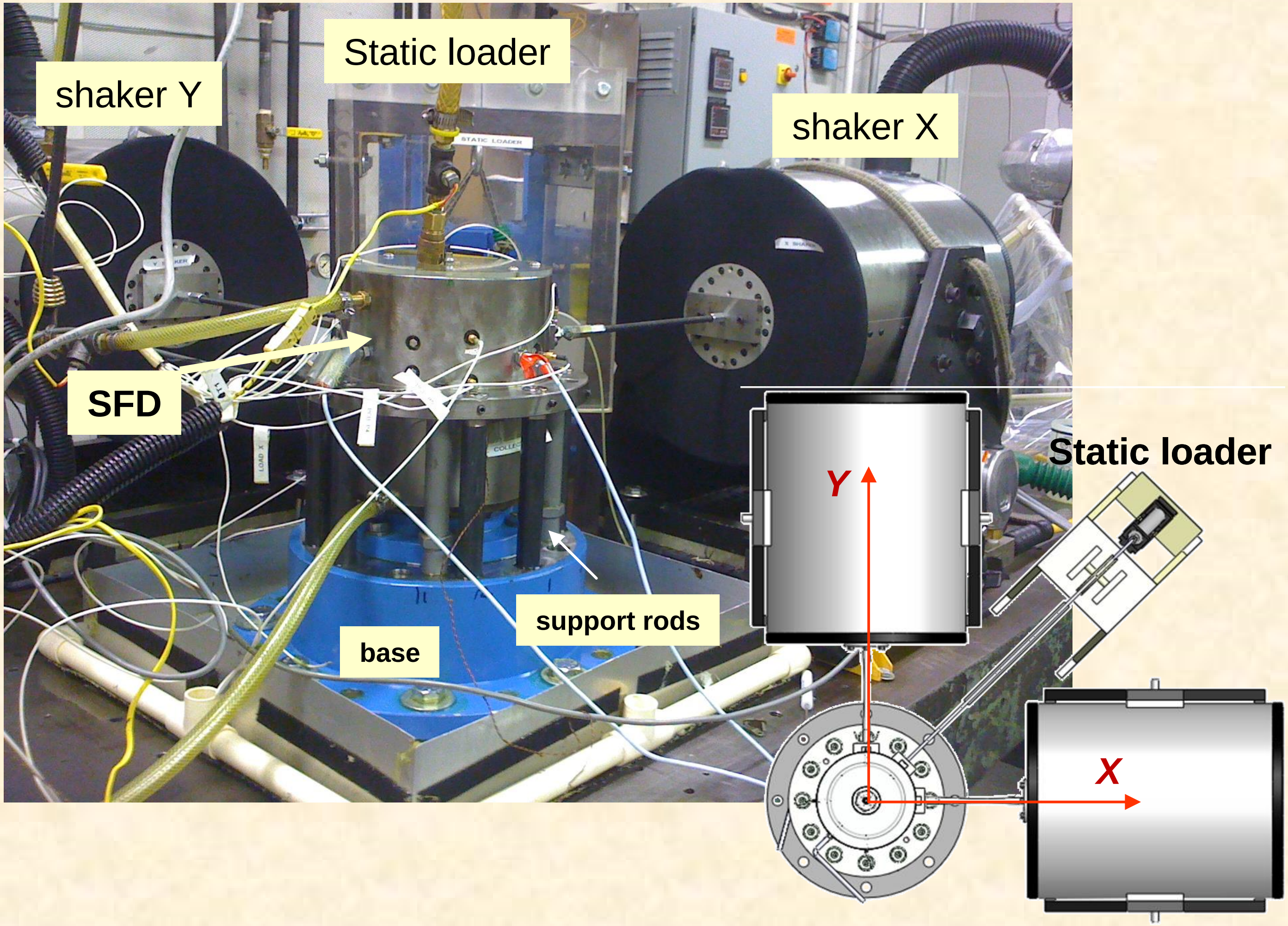

Lubricant flow path

ISO VG 2 oil

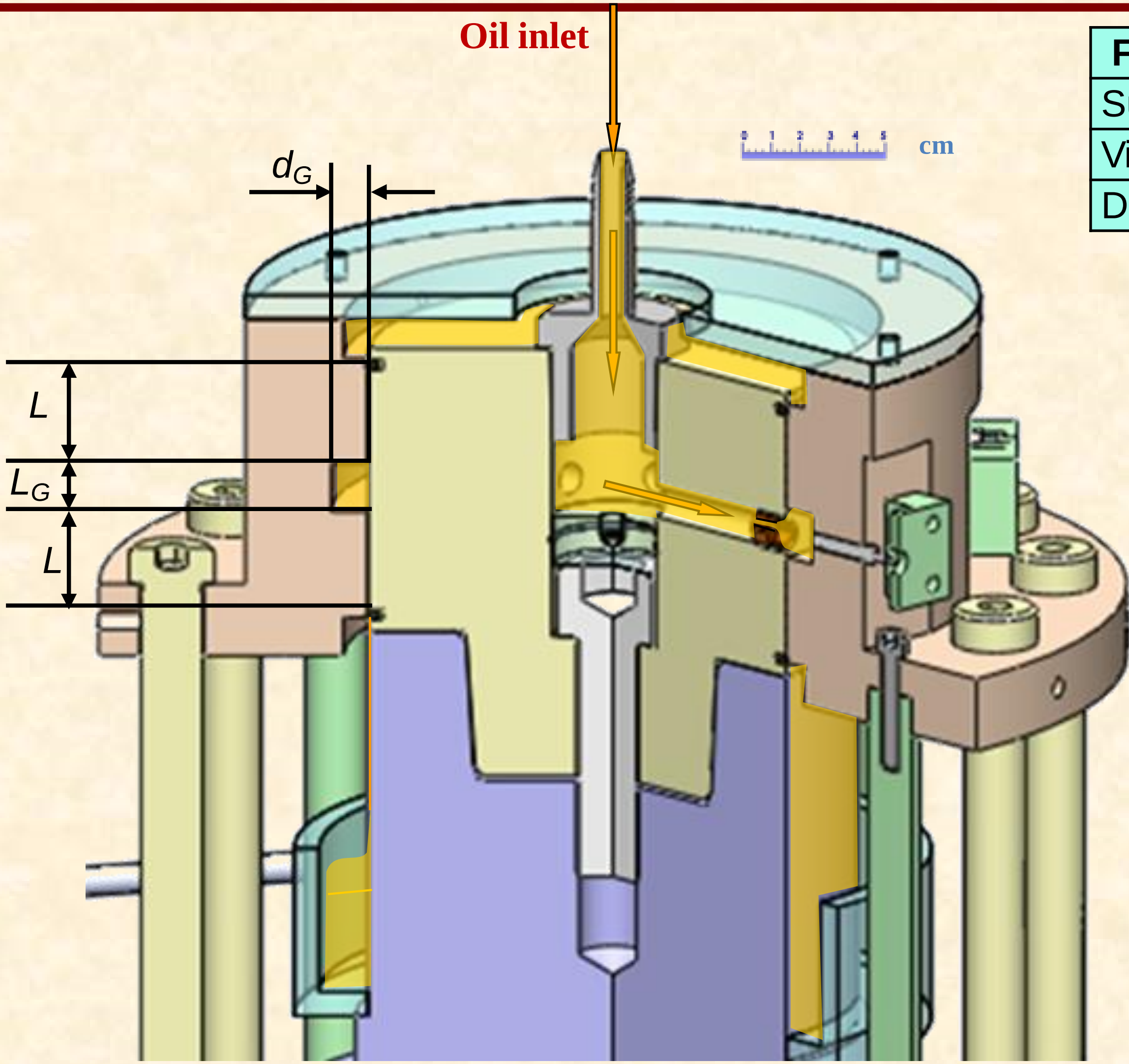

Fluid properties ISO VG2	
Supply temperature (T_{in})	25 ^oC
Viscosity	2.96 c-Poise
Density	785 kg/m^3

	Long journal (A)	Short journal (B)
Land length (L)	25.4mm	12.7mm
Land clearance (c)	0.14 mm	0.13 mm

Journal diameter (D)	12.7cm
Groove length (L_G)	12.7 mm
Groove depth (d_G)	9.52 mm

Multiple-year test program (2008- 2018)

Damper A (c_A=140 µm (5.5 mil))

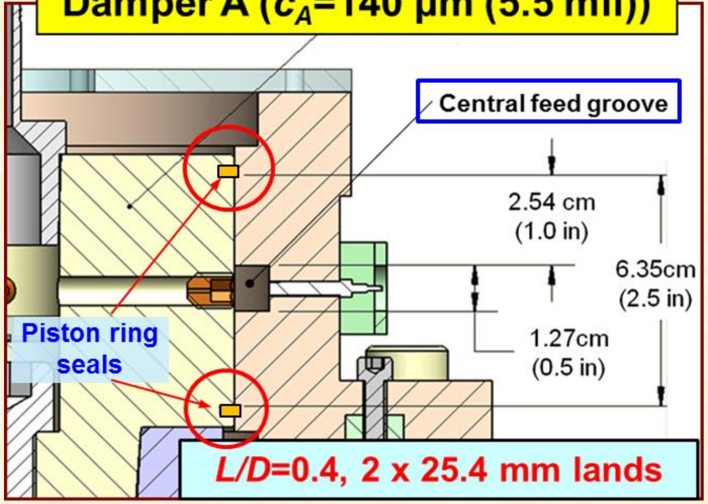

Damper B (c_B=137 µm (5.4 mil))

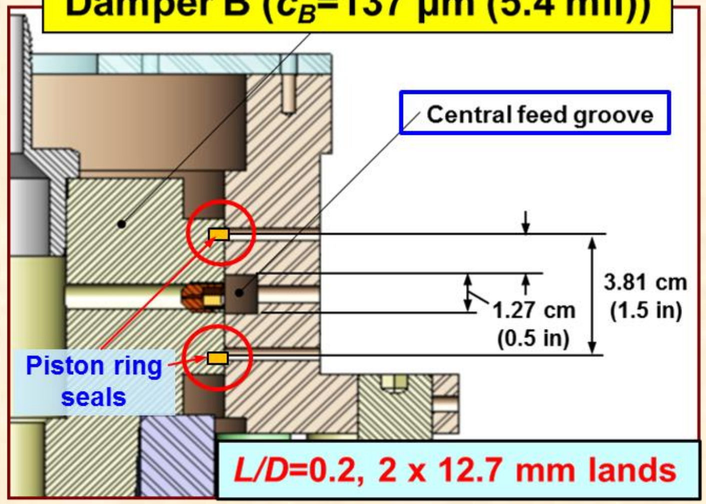

Damper C (c_C=130 µm (5.1 mil))

Damper D (c_D=254 µm (10.0 mil))

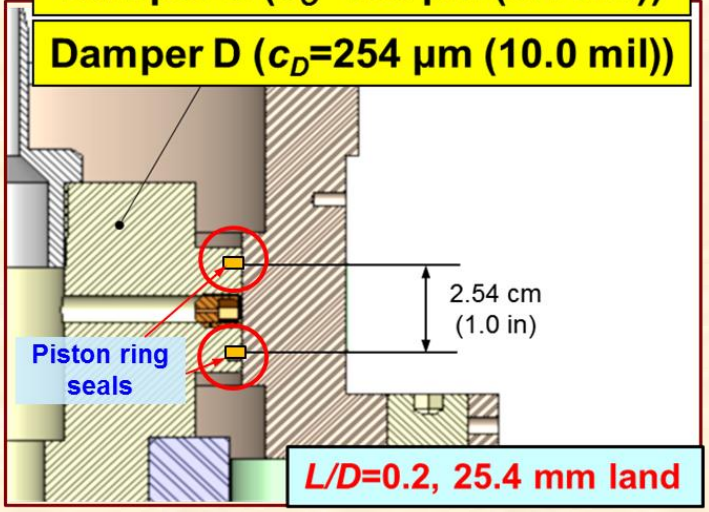

Damper E (c_E=122 µm (4.8 mil))

Damper F (c_F=267 µm (10.5 mil))

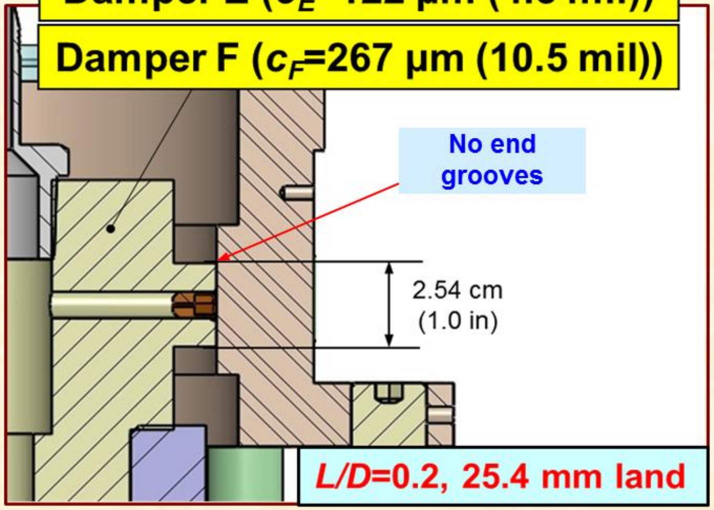

Objective:
Optimize SFD influence on rotor dynamics.

Identification of SFD force coefficients

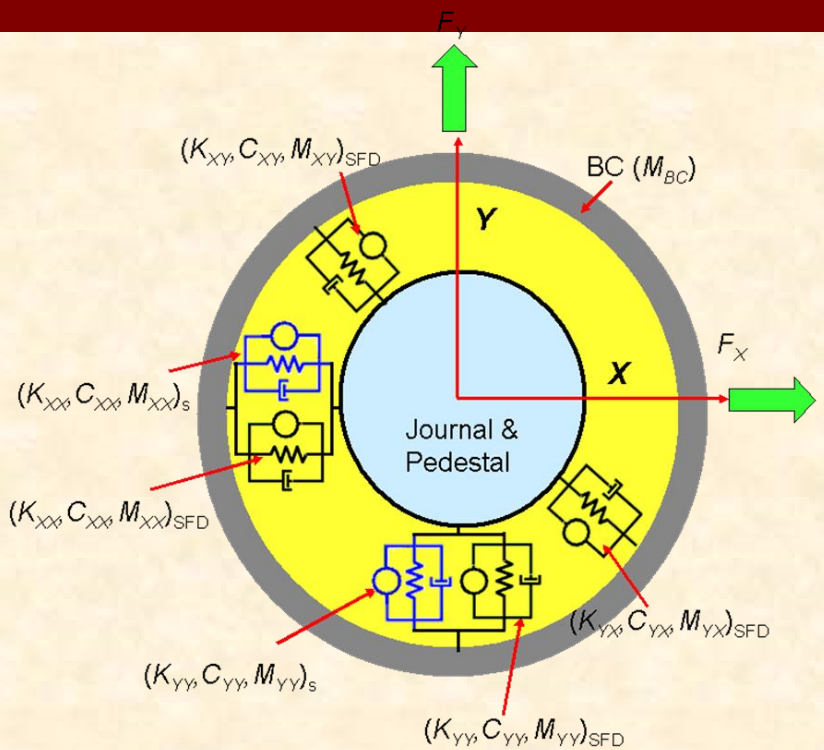

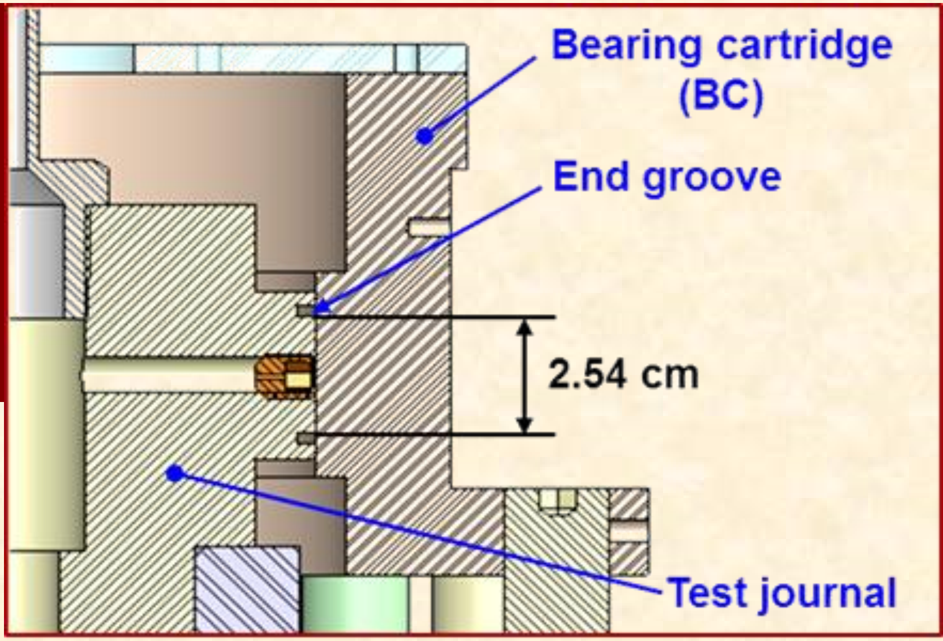

Test procedure

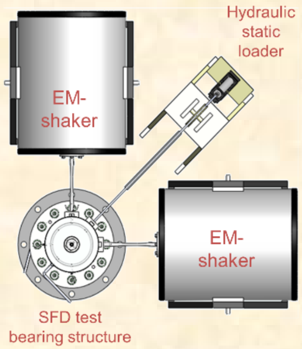

Evaluate SFD force coefficients from whirl orbits: amplitude (*r*) grows with offset or static eccentricity (e_s) – 45° away.

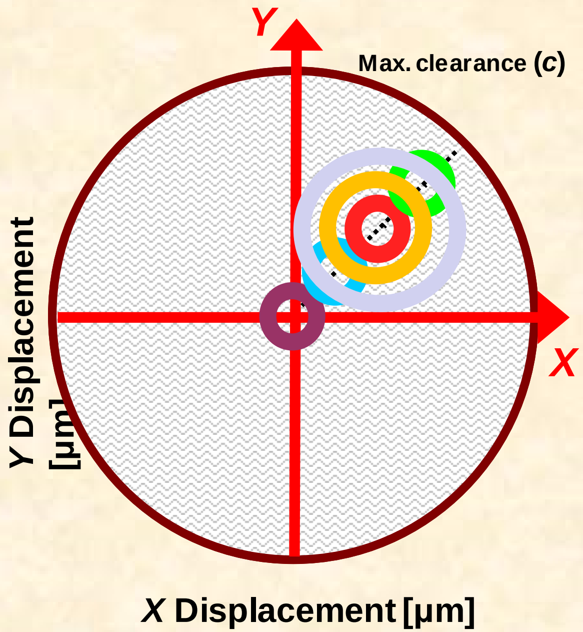

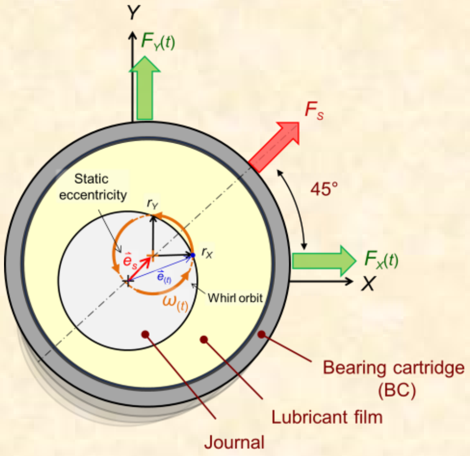

(1) Apply loads → record BC motions

Shakers apply forces

$$\mathbf{F}^1 = \mathrm{Re}\left(\begin{bmatrix} F_X{}^1 \\ iF_Y{}^1 \end{bmatrix} e^{i\omega t}\right)$$

$$\mathbf{F}^2 = \mathrm{Re}\left(\begin{bmatrix} F_X{}^2 \\ -iF_Y{}^2 \end{bmatrix} e^{i\omega t}\right)$$

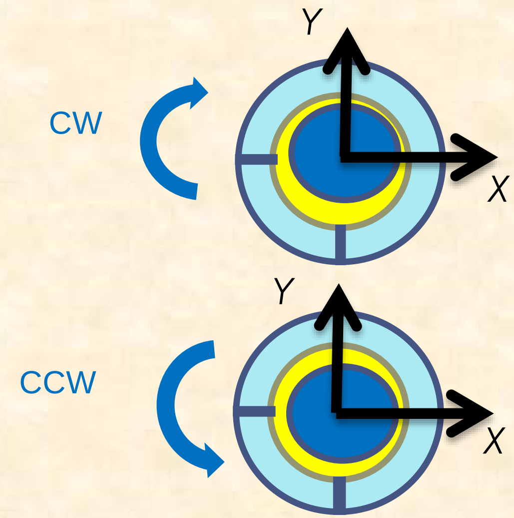

Record BC displacements and accelerations

$$\mathbf{z}^1 = \begin{bmatrix} x^1_{(t)} \\ y^1_{(t)} \end{bmatrix} = \begin{bmatrix} X^1 \\ Y^1 \end{bmatrix} e^{i\omega t}$$

$$\mathbf{a}^1$$

$$\mathbf{z}^2 = \begin{bmatrix} x^2_{(t)} \\ y^2_{(t)} \end{bmatrix} = \begin{bmatrix} X^2 \\ Y^2 \end{bmatrix} e^{i\omega t}$$

$$\mathbf{a}^2$$

Load $\mathbf{F}_{(t)}$, displacement $\mathbf{z}_{(t)}$ and acceleration $\mathbf{a}_{(\mathrm{t})}$ recorded at each frequency

EOM: Frequency Domain

$$[\mathbf{K_L} + i\omega\mathbf{C_L} - \omega^2\mathbf{M_L}]\bar{\mathbf{z}} = \bar{\mathbf{F}} - M_{BC}\bar{\mathbf{a}}$$

$$\rightarrow \mathbf{H_L z}$$

Unknown Parameters:

$$\mathbf{K_L}, \mathbf{C_L}, \mathbf{M_L}$$

Identification of parameters

Step 2 : Transform to frequency domain and curve fit H_L's

Complex dynamic stiffness

***r/c$_A$*=0.2**

$$\mathrm{Re}\left([\bar{\mathbf{F}} - M_{BC}\bar{\mathbf{a}}]\bar{\mathbf{z}}^{-1}\right) \rightarrow \mathbf{K}_\mathbf{L} - \omega^2 \mathbf{M}_\mathbf{L}$$

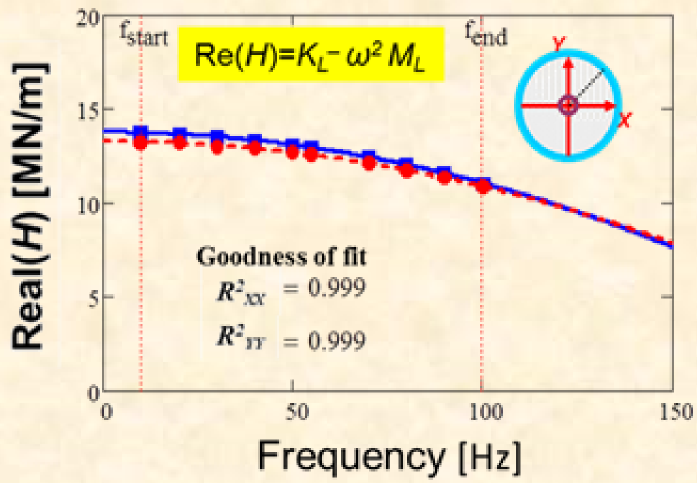

$$\mathrm{Im}\left([\bar{\mathbf{F}} - M_{BC}\bar{\mathbf{a}}]\bar{\mathbf{z}}^{-1}\right) \rightarrow \mathbf{C}_\mathbf{L}\omega$$

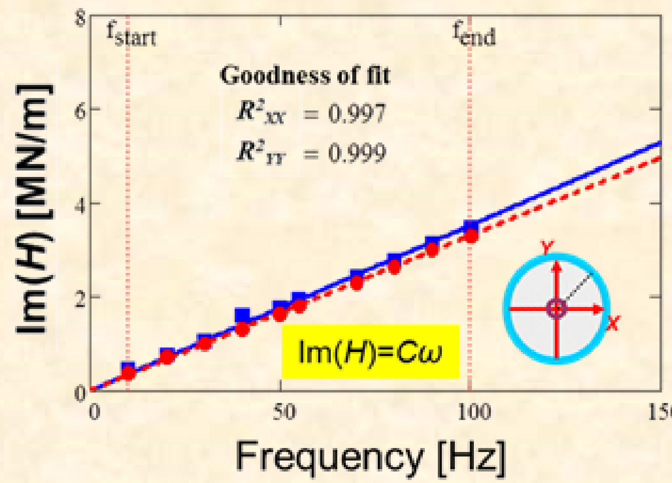

Physical model Re(H_{XX}) → K-$\omega^2 M$ and Im(H_{XX})→ $C\omega$ agree well with experimental data.
Damping C is constant over frequency range

SFD coefficients

$$(K, C, M)_{SFD} = (K, C, M)_L - (K, C, M)_S$$

SFD Test system (lubricated) Dry structure

Force coefficients for two open ends SFDs

1 inch land (*L/D*=0.20)
Clearance:
***c*=small (5 mil) vs. large (10 mil)**

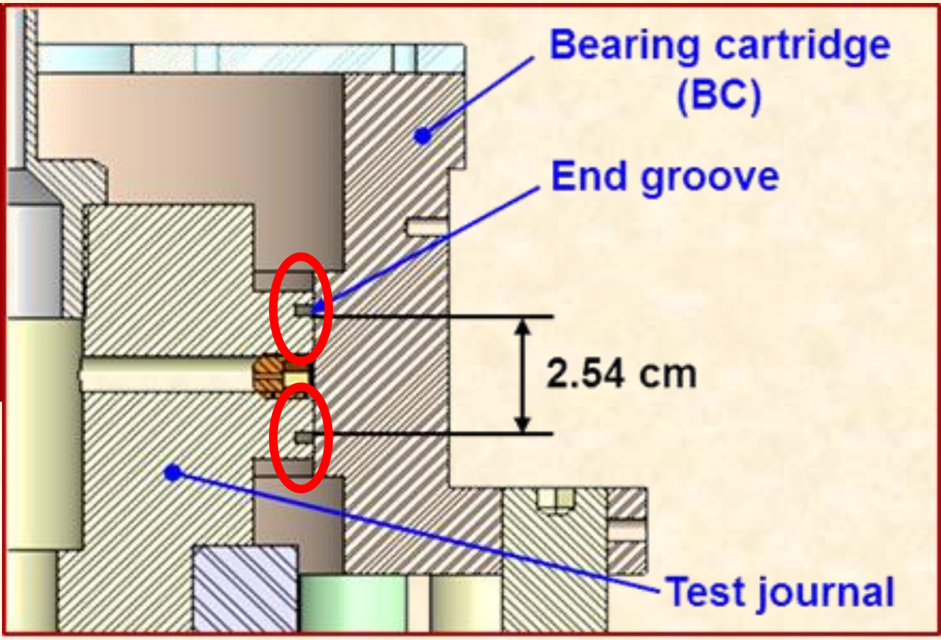

SFD test bearing and film geometry

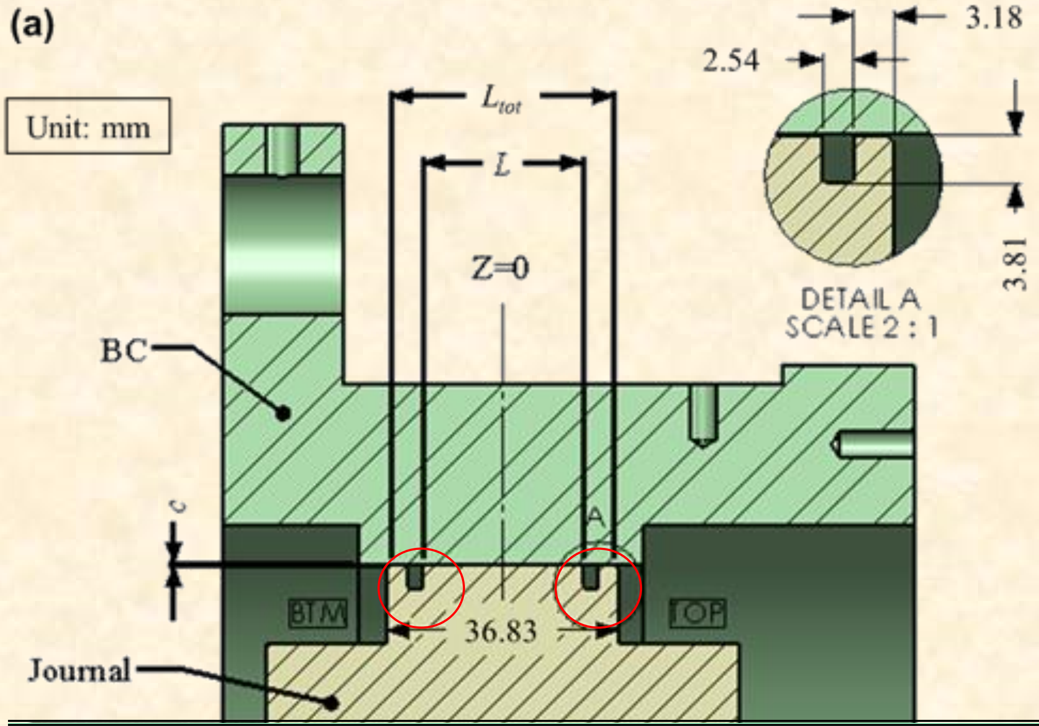

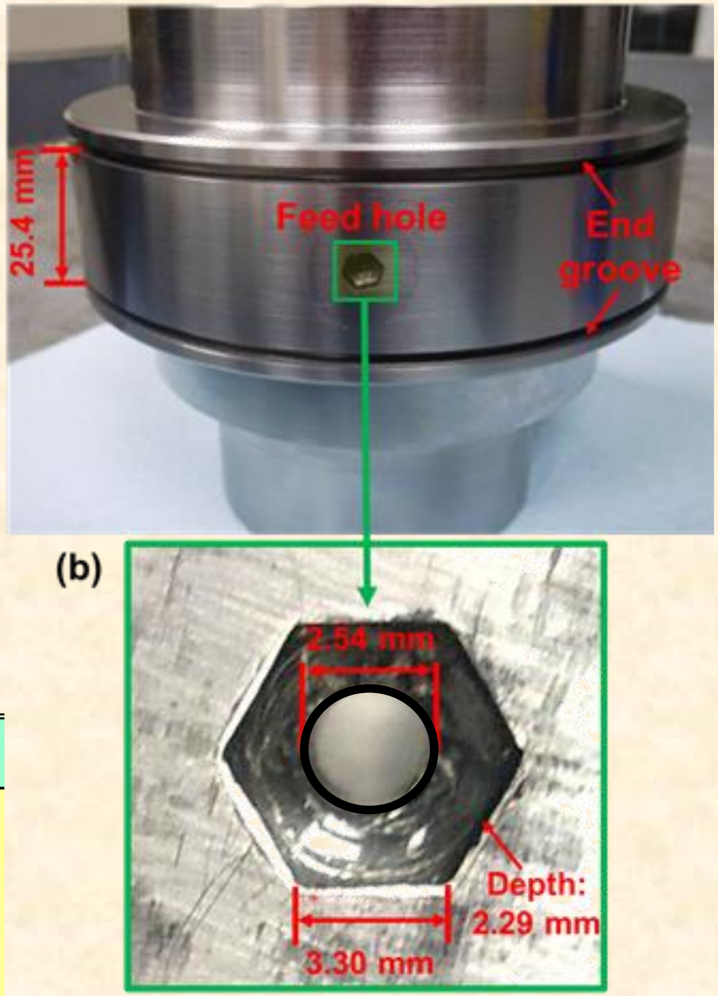

Geometry of SFD	A	B
Film land length, L (mm)	25.4	
Radial clearance, c_A , c_B (mm)	0.129	0.254
End grooves: depth × width (mm)	3.8 × 2.5	
Total wetted length, L_{tot} (mm)	36.8	

Normalization of force coefficients

Force coefficients normalized to magnitudes from classical formulas (prior slide):

$$\bar{C} = {C}/{C^*} \qquad \bar{M} = {M}/{M^*}$$

Damper A $c_A = 0.129$ mm	$C^*_A = 6.01$ kN.s/m, $M^*_A = 2.69$ kg
Damper B $c_B = 0.254$ mm	$C^*_B = 0.95$ kN.s/m, $M^*_B = 1.37$ kg

$\bar{C} \sim 1$ & $\bar{M} \sim 1$ **denote <u>one to one</u> agreement with predictive formulas.**

Damper A (c_A = 129 μm) – damping coeffs.

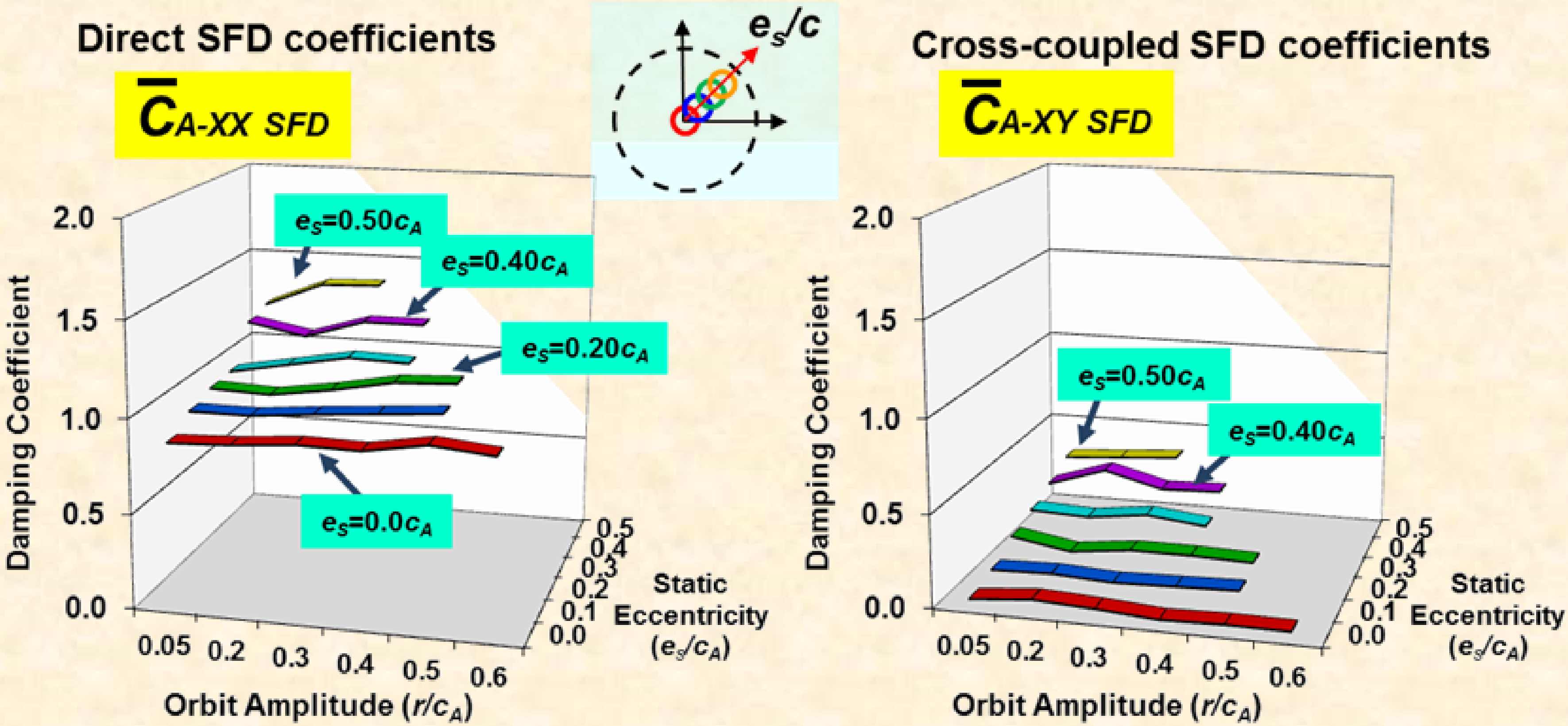

$C_{XX} \sim C_{YY}$

Findings: **Damping** coefficients **increase** with increasing **orbit amplitude** and **static eccentricity**. At $r/c_A \leq 0.2, \bar{C}_{A-xx}$ ~ **0.85.**

Damper A (c_A = 129 μm) added mass coeffs.

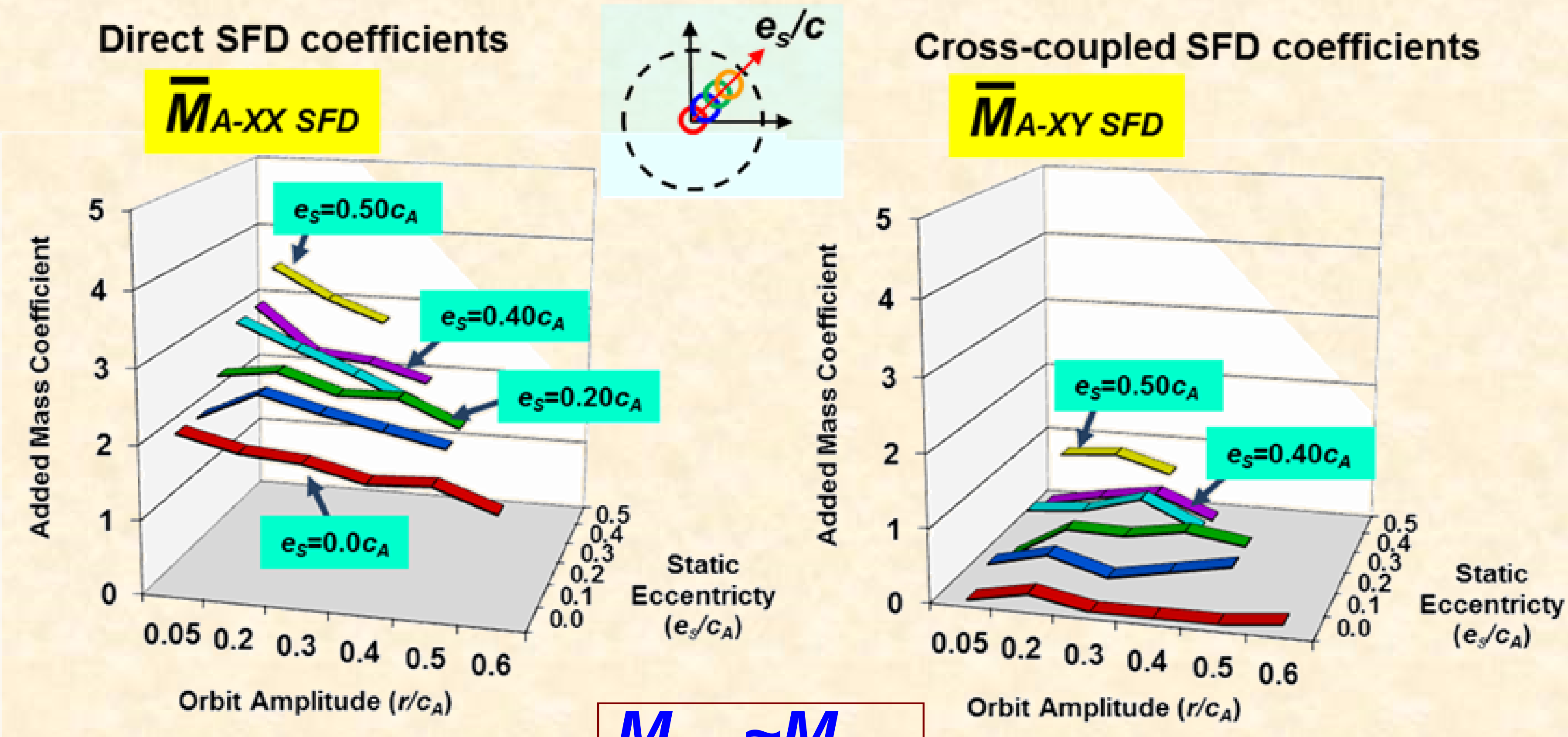

$M_{XX} \sim M_{YY}$

Findings: **Added mass** coefficients **increase** with increasing **static eccentricity**; but **decrease** with increasing **orbit amplitude**. **Theory under predicts inertia coefficient, even for small amplitude motions.**

Compare damping coeffs. of two dampers

$$\hat{C} = C \Big/ C_{B(r/c_B=0.15)}$$

$e_S/c=0$

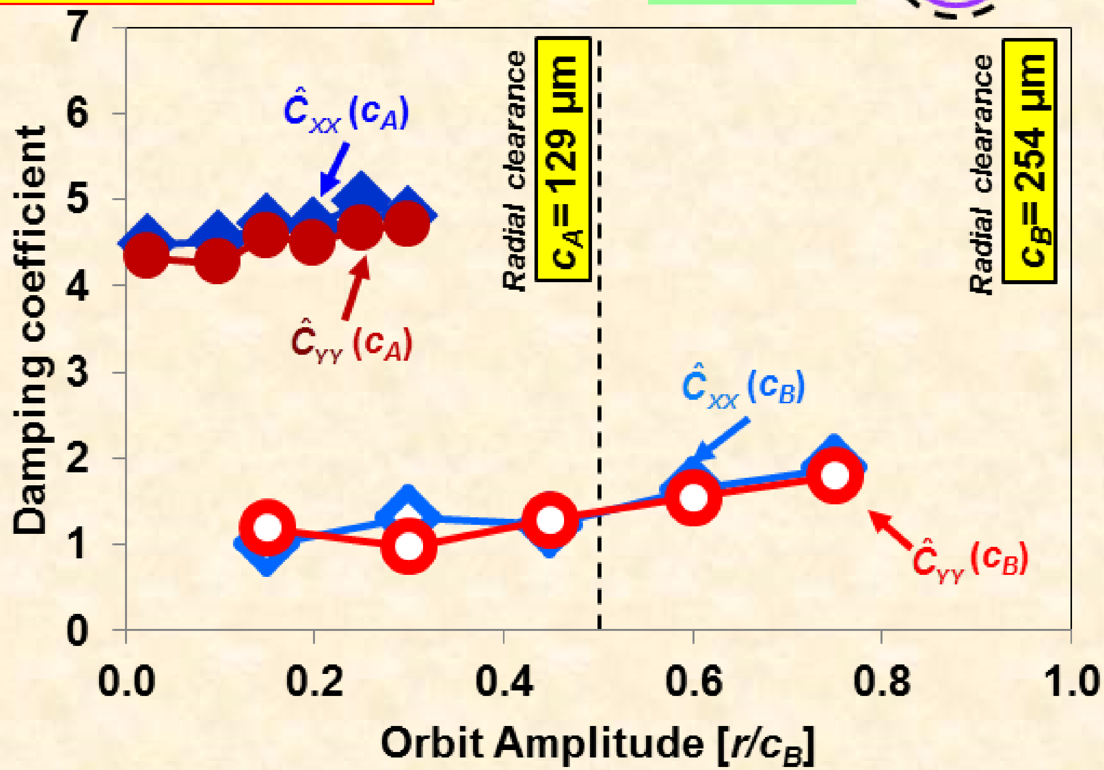

Damper A	Damper B
c_A=0.129 mm	c_B=0.254 mm

Recall ➡ $C \sim \mu \left(\frac{1}{c}\right)^3$

$$\left(\frac{c_B}{c_A}\right)^3 \left(\frac{\mu_A}{\mu_B}\right) = \left(\frac{0.25}{0.13}\right)^3 \left(\frac{2.5}{2.7}\right) = 6.9$$

Damping coefficients for small film clearance (c_A) damper are **~4 times larger** than the coefficients obtained with larger clearance (c_B) SFD.

Compare **inertia** coeffs. of two dampers

$$\hat{M} = \frac{M}{M_{B(r/c_B=0.15)}}$$

$e_S/c=0$

Damper A	Damper B
c_A=0.129 mm	c_B=0.254 mm

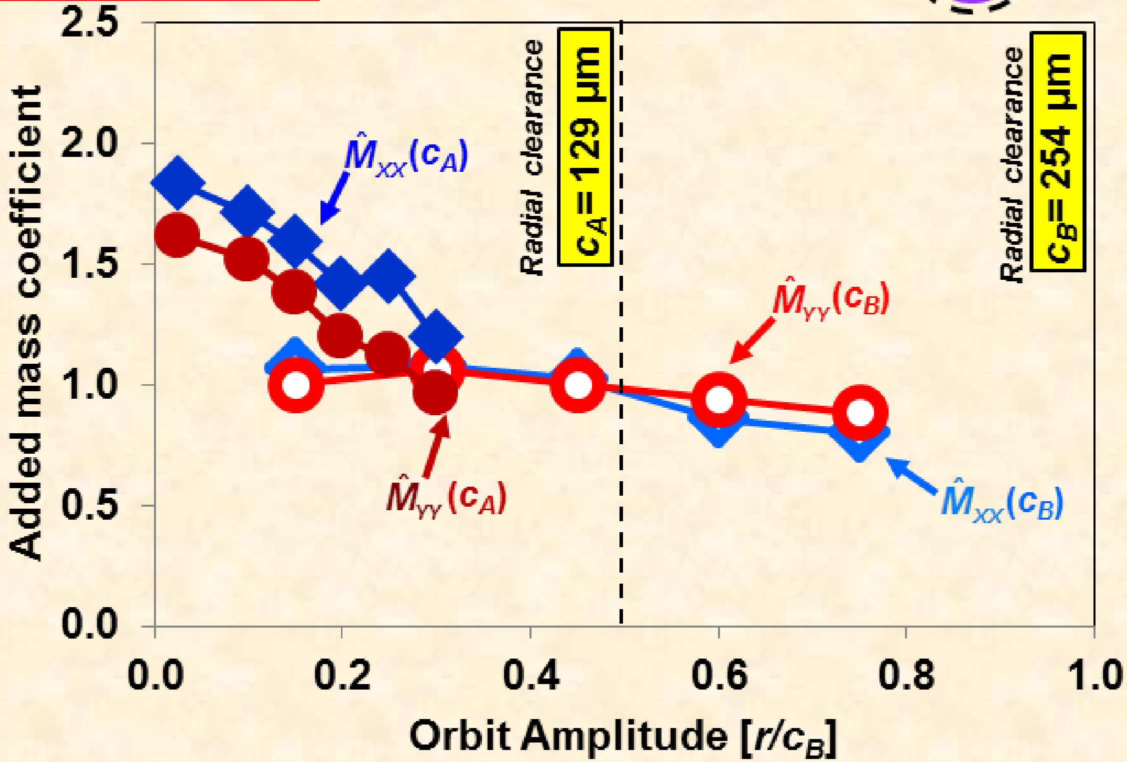

Recall $M \sim \left(\frac{1}{c}\right)$

$$\left(\frac{c_B}{c_A}\right) = \left(\frac{0.25}{0.13}\right) = 1.96$$

Added mass coefficients for the small film clearance (c_A) damper are **~1.8 times higher** than the coefficients obtained with larger clearance (c_B) SFD.

Closure I: open ends SFD GT2015-43096

From circular orbit tests

Damper A	Damper B
c_A=0.129 mm	c_B=0.254 mm

(a) For both dampers, **direct damping** coefficients do not show + sensitivity to the size of the orbit radius (*r*).

(b) **Inertia** coefficients for the large clearance damper B are **insensitive** to orbit amplitude (*r*), while small clearance damper A shows added masses **decreasing** with orbt size (*r*).

SFD force coefficients
Comparison between short and long <u>open ends</u> dampers with a central groove

Long: 2 x 25.4 mm lands

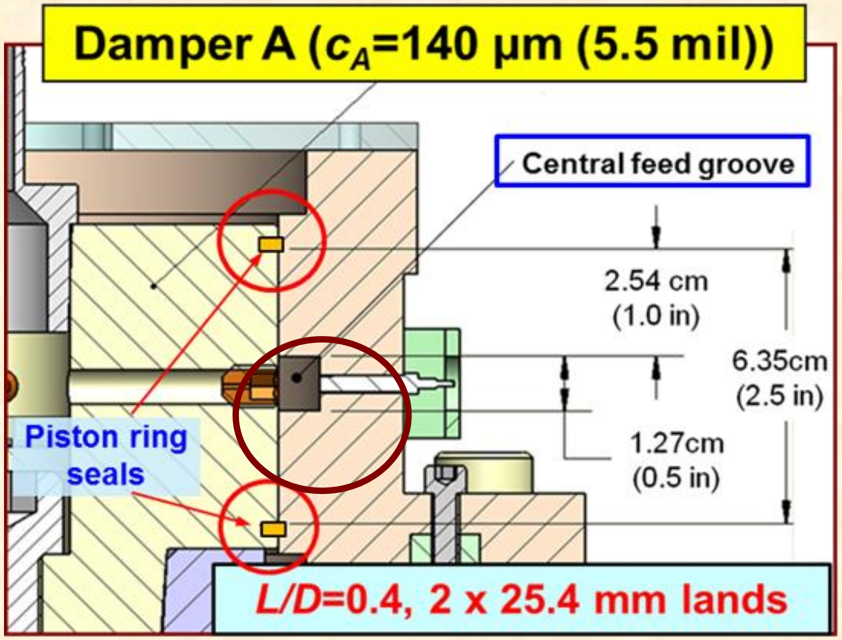

Short: 2 x12.7 mm lands

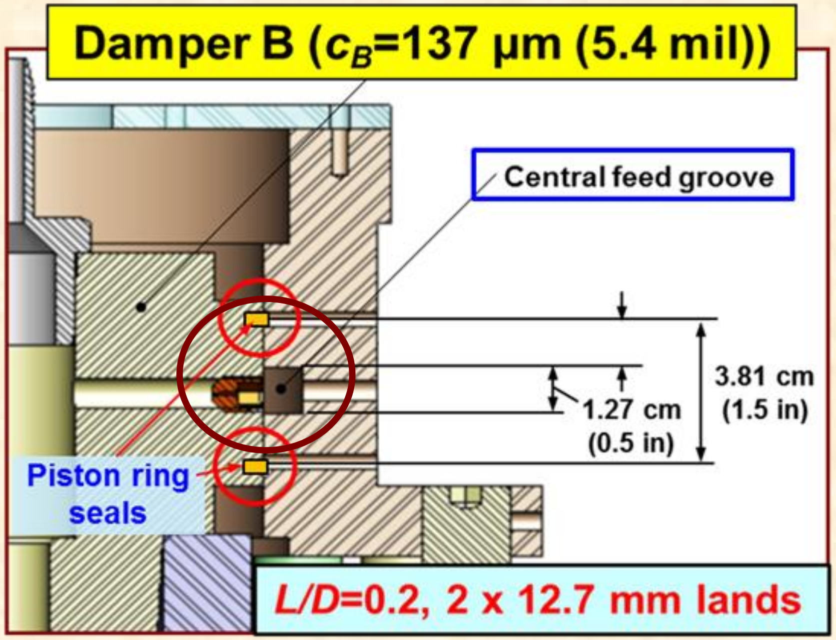

Generation of dynamic pressure in film and groove

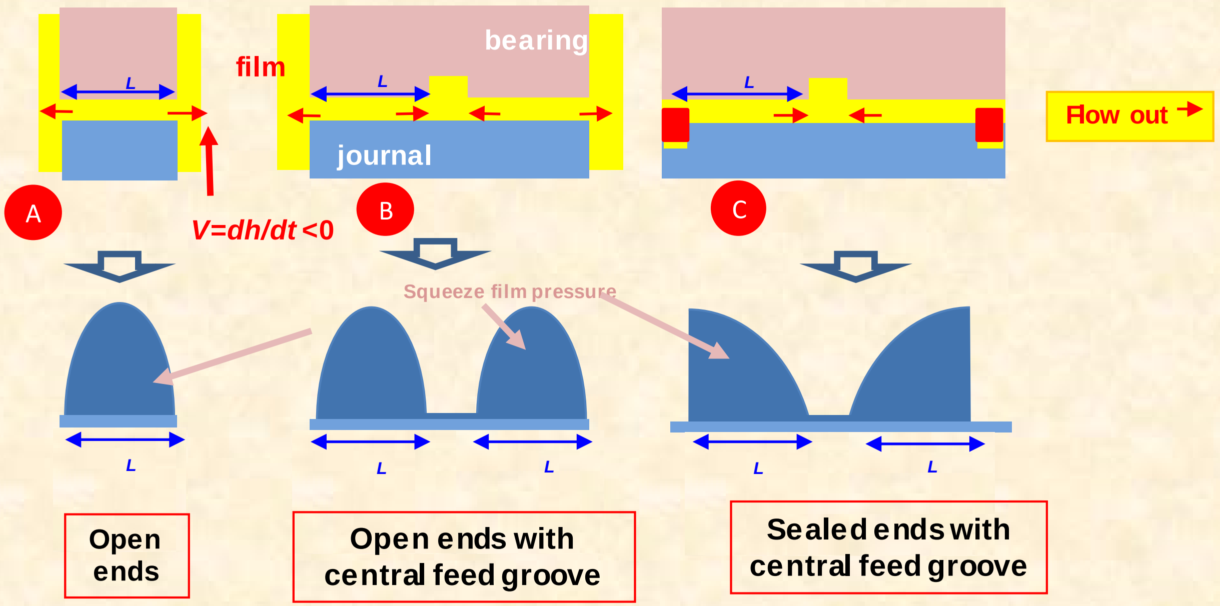

Conventional knowledge:
A groove has constant pressure

Does a (deep) central groove isolate a damper into two independent halves?

Generation of dynamic pressure in a groove

Measured:

Does a central groove isolate a damper into two independent halves?

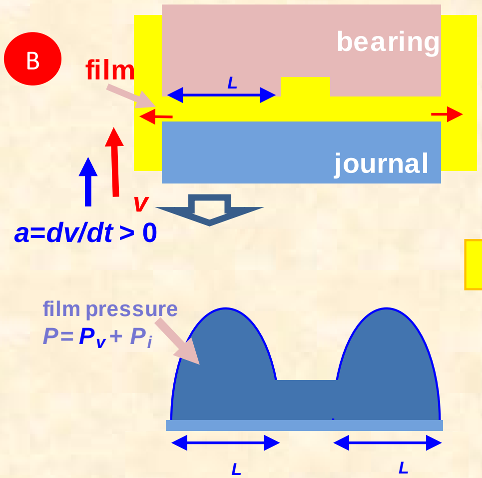

Open ends with central feed groove

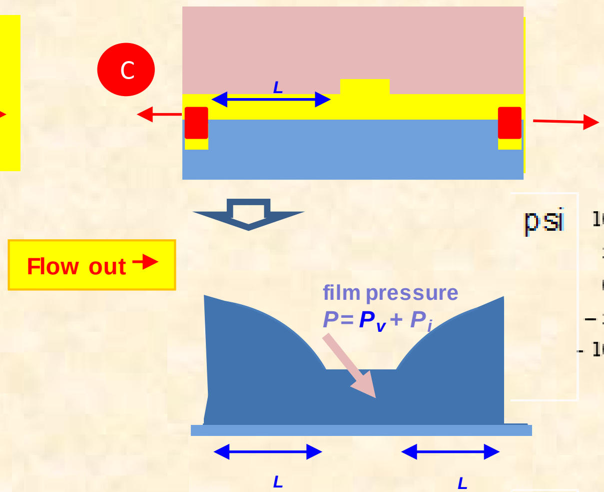

Sealed ends with central feed groove

Film land

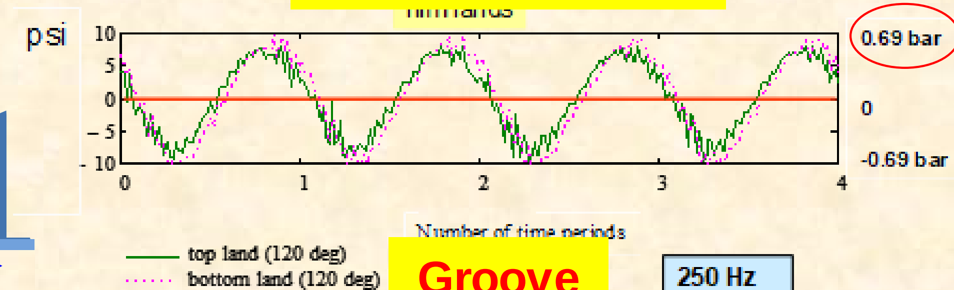

Groove

250 Hz

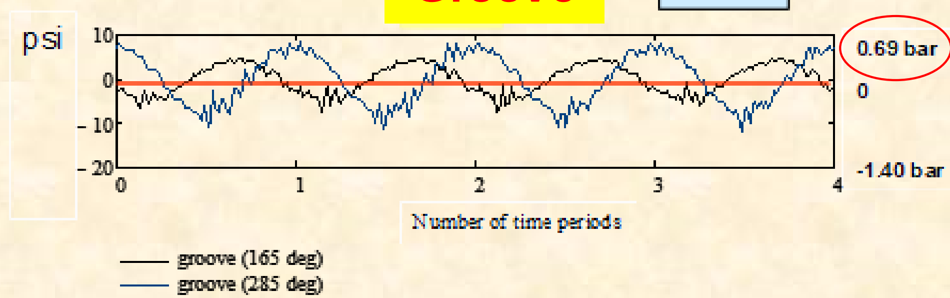

No! grooves produce squeeze film pressures!

compare SFD damping

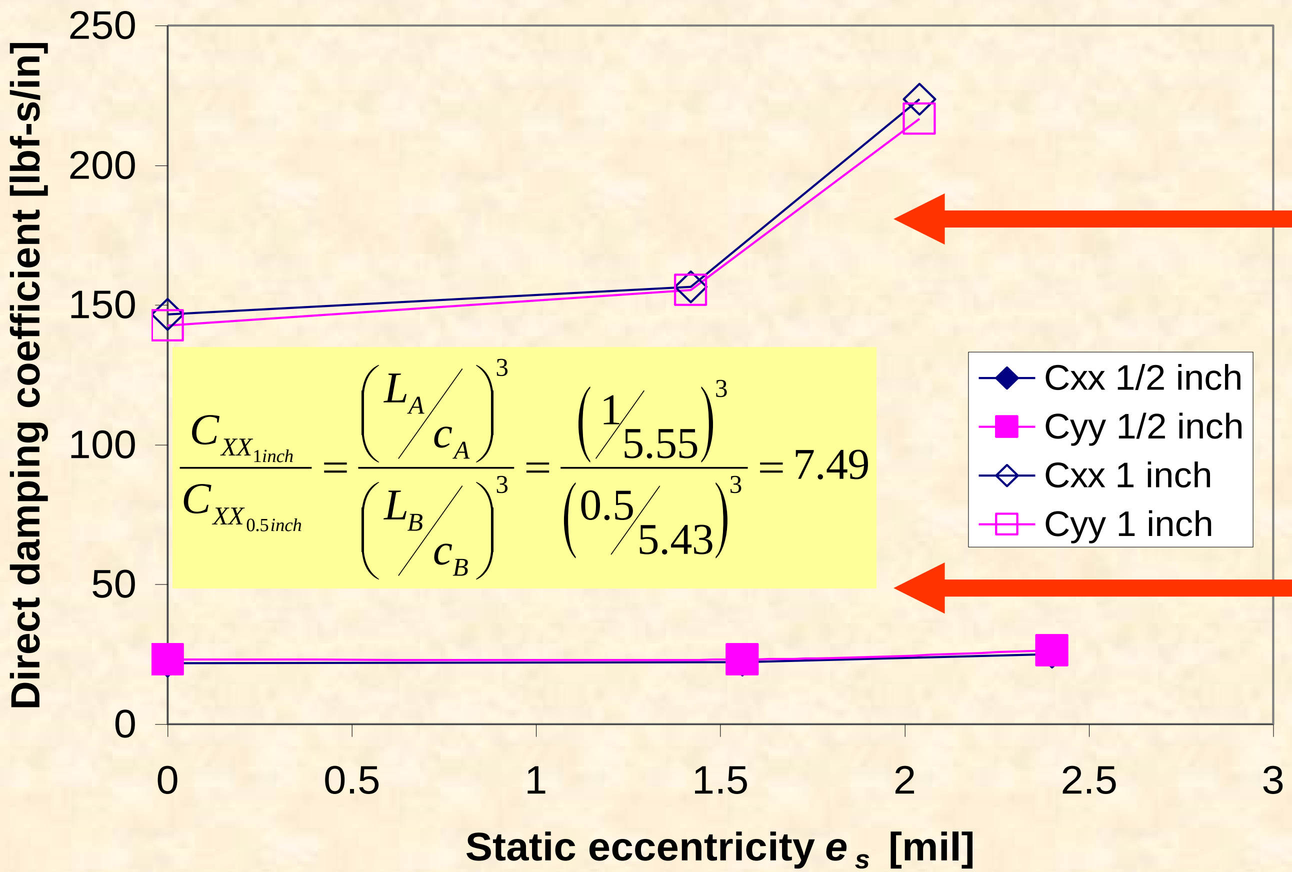

$$\frac{C_{XX_{1inch}}}{C_{XX_{0.5inch}}} = \frac{\left(L_A / c_A\right)^3}{\left(L_B / c_B\right)^3} = \frac{\left(1 / 5.55\right)^3}{\left(0.5 / 5.43\right)^3} = 7.49$$

$C_{XX} \sim C_{YY}$

Long (L=1 inch)

$C_{XX} \sim C_{YY}$

Short (L=0.5 inch)

Ratio of coefficients ~ (L/c^3)

Long and short SFDs (circular orbits)

compare SFD inertia

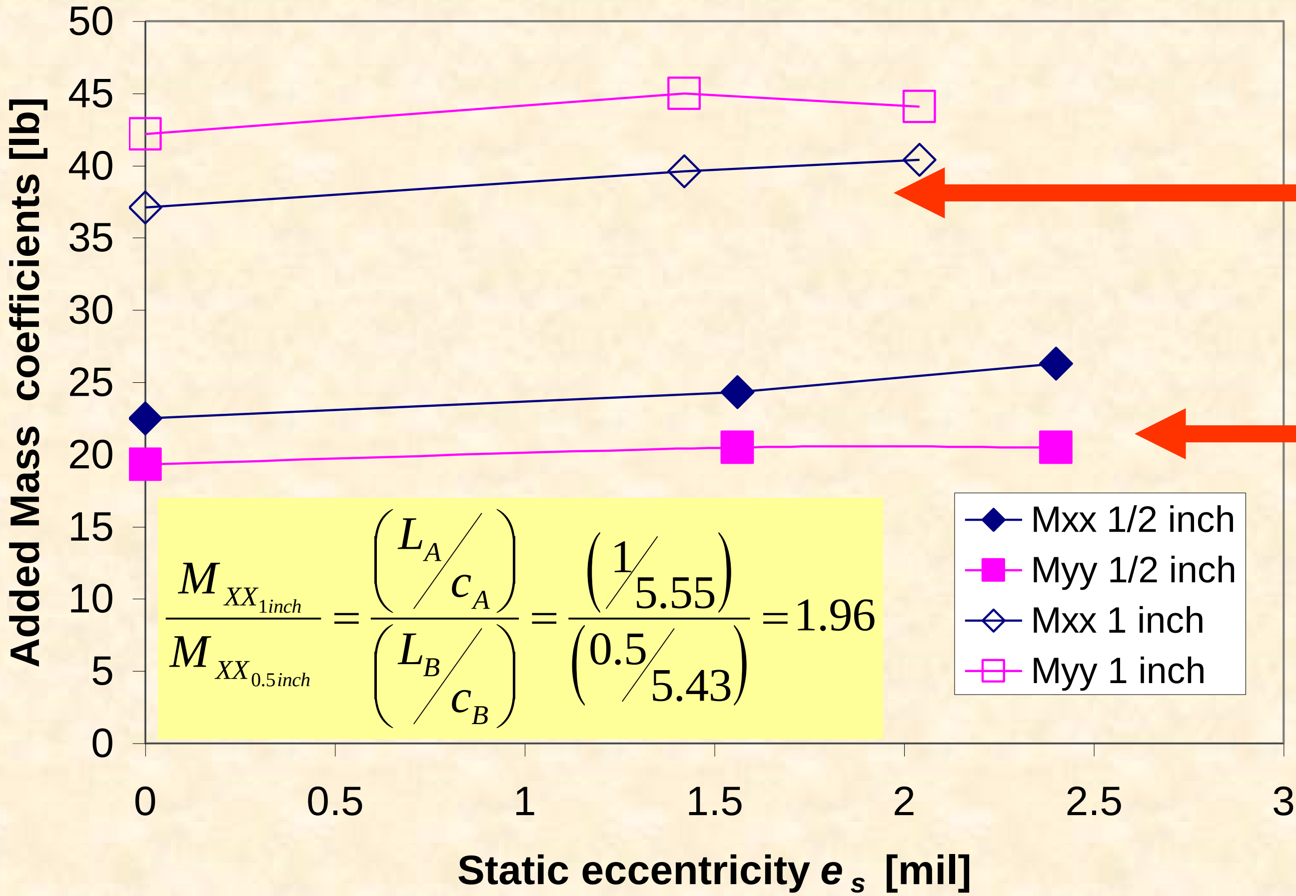

$$\frac{M_{XX_{1inch}}}{M_{XX_{0.5inch}}} = \frac{\left(L_A / c_A\right)}{\left(L_B / c_B\right)} = \frac{\left(1/5.55\right)}{\left(0.5/5.43\right)} = 1.96$$

M_{XX} , M_{YY}
Long (L=1 inch)

M_{XX} , M_{YY}
Short (L=0.5 inch)

Ratio of coefficients ~ (L/c)

Long and short SFDs (circular orbits)

Closure II: Long vs short SFDs

Open ends long damper shows ~ 7 times more damping than short length damper. Inertia coefficients are twice larger.

SFD force coefficients are more a function of static eccentricity (max. 2 mil) than amplitude of whirl & changing little with ellipticity of orbit.

For all damper configurations and most test conditions: cross-coupled damping and inertia force coefficients are small.

Experimental SFD force coefficients
Comparison open ends & sealed ends long (1”) SFD

Damper A (c_A=140 μm (5.5 mil))

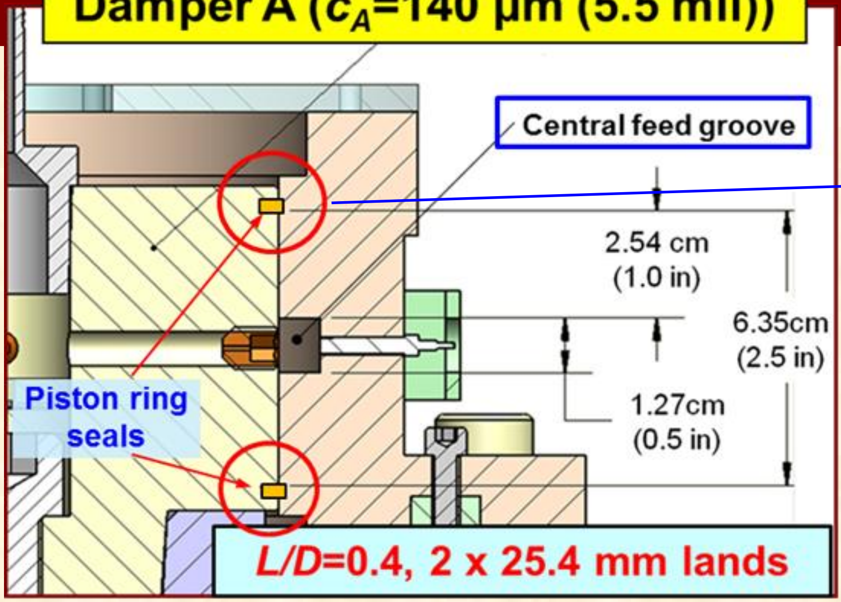

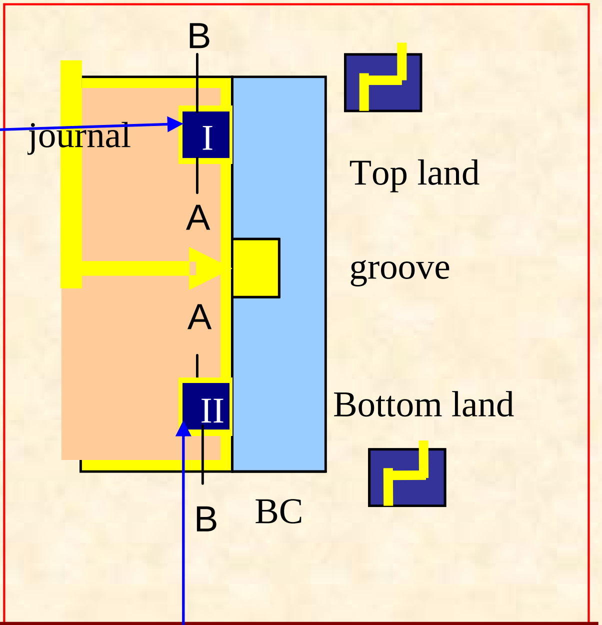

compare SFD damping

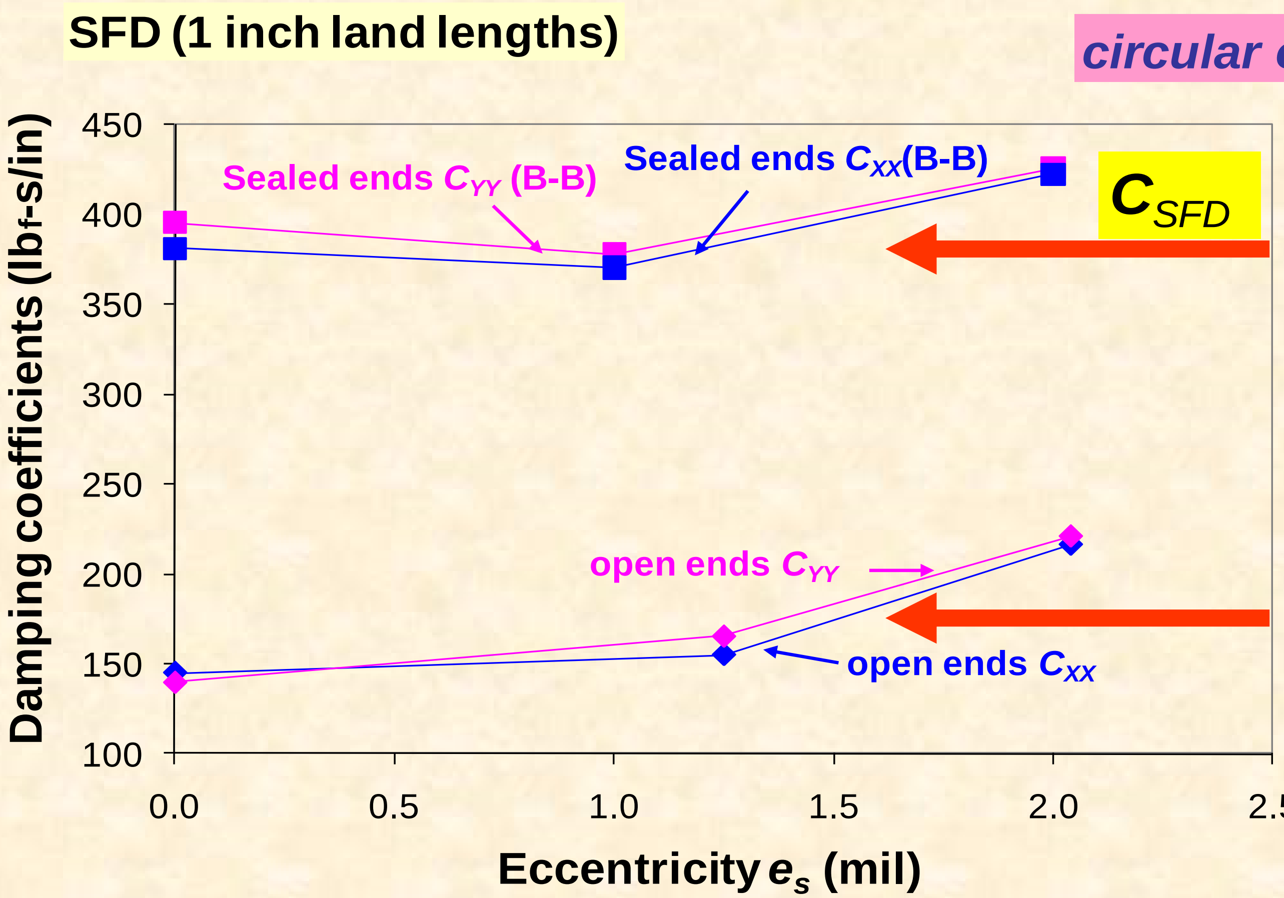

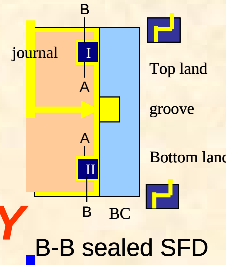

C_{XX} ~ C_{YY}

Sealed ends

C_{XX} ~ C_{YY}

Open ends

Open ends vs sealed ends (circular orbits)

compare SFD inertia

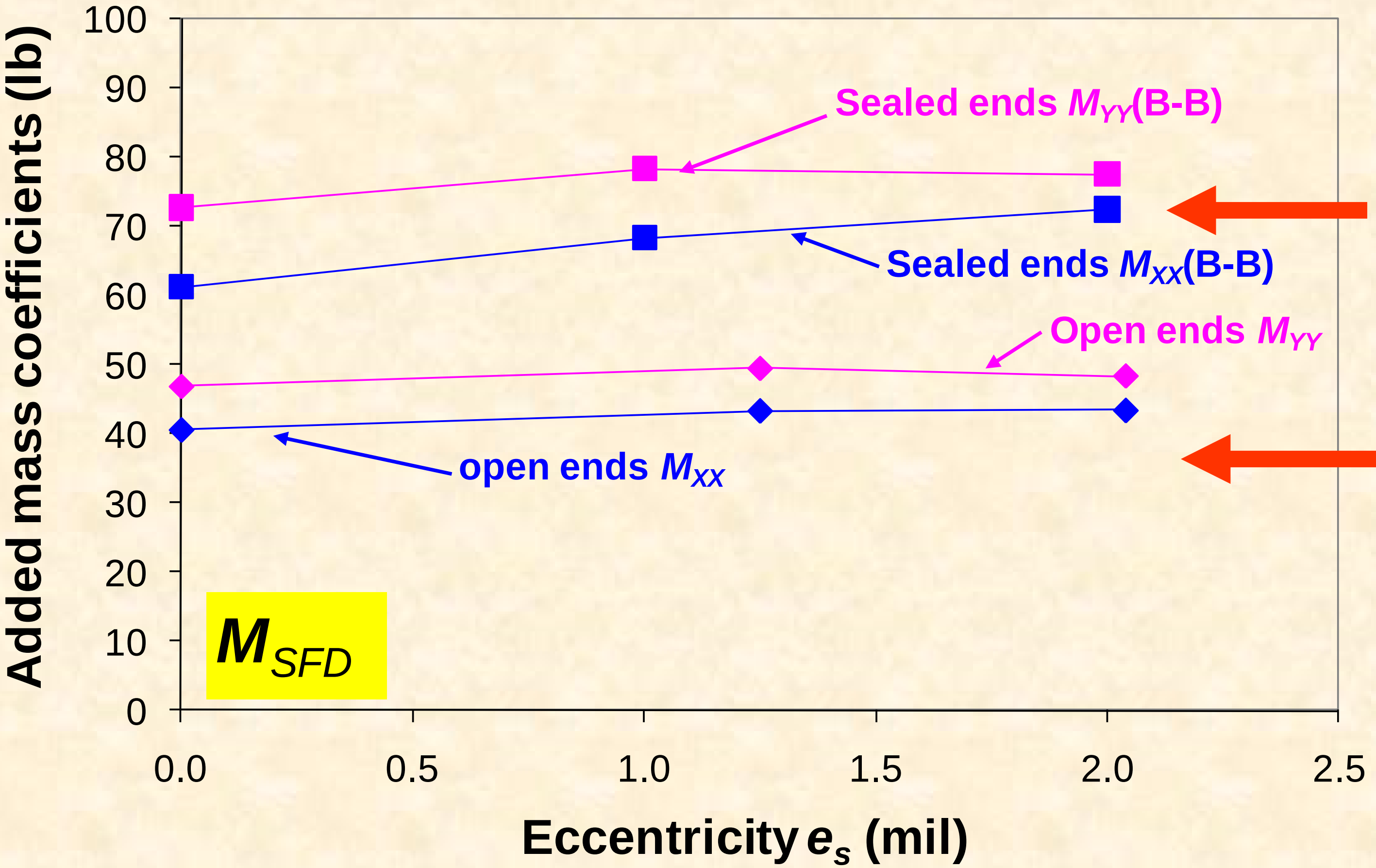

M_{XX} , M_{YY}
Sealed ends

M_{XX} , M_{YY}
Open ends

Open ends vs sealed ends (circular orbits)

Closure III: Open vs Sealed SFDS

Sealed ends long damper has ~ 3 times more damping than <u>open ends damper</u>. Inertia coefficients are 1.5 times larger.

SFD force coefficients are more a function of static eccentricity (max. 50 micro-m) than of the amplitude of whirl. Coefficients change little with ellipticity of orbit (up to 5:1 ratio)

Proper installation of piston rings is crucial for adequate sealing.

Oil cavitation OR air ingestion in SFDs?

Cavitation in liquid bearings

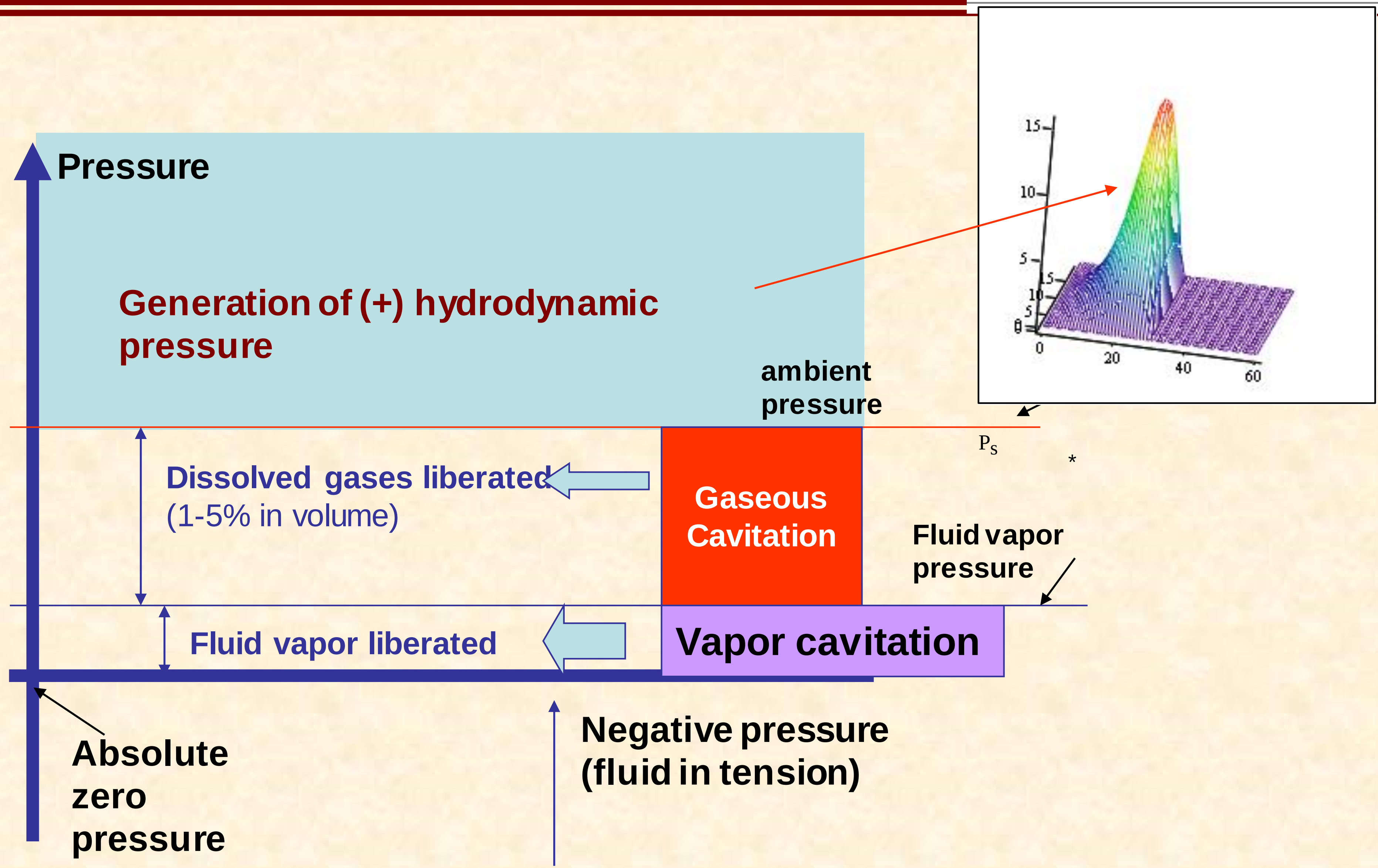

Cavitation in oil lubricated bearings

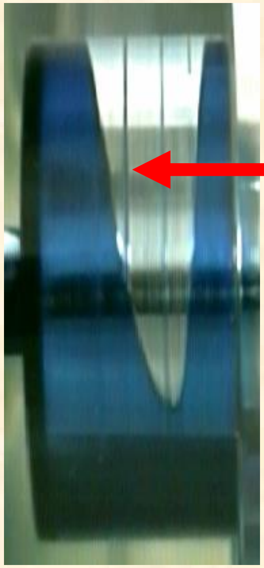

Pressure is uniform (constant) inside cavitation “bubble” – Flow reformation at trailing edge of bubble

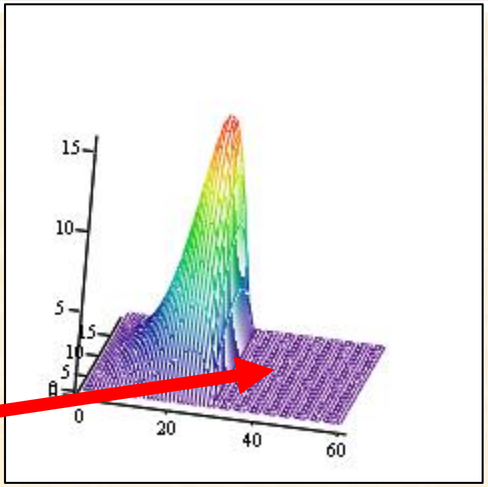

P_S *

But… air ingestion & entrainment persist under dynamic load conditions.

Classical cavitation models do not apply to air entrainment under dynamic loading.

SFD Operation Issue

Air ingestion and entrapment

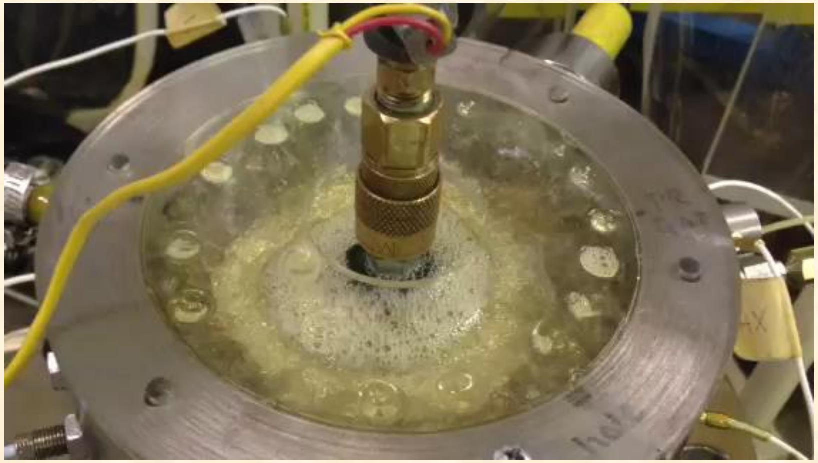

Bubbly lubricant exits from top and bottom ends of damper

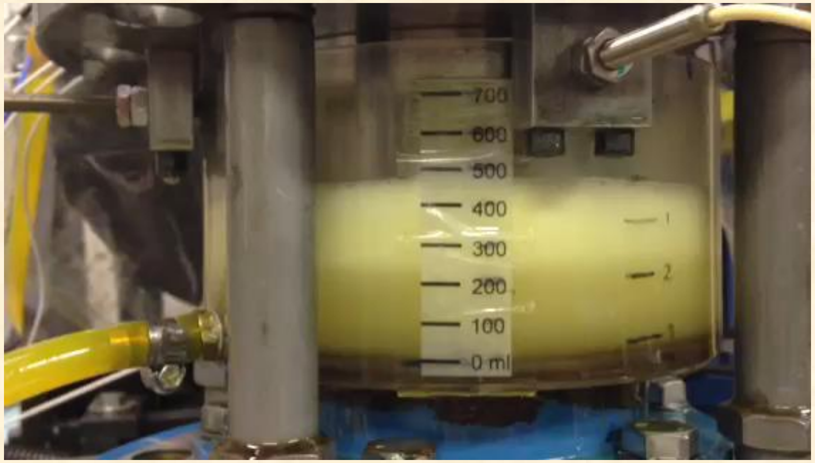

Onset of air ingestion

Sealed ends SFD

Oil foamy mixture evolves from lubricant exiting through piston ring slit.

After 10 years of continued work,

what did we learn?

Conclusion (1):

(a) Damping (*C*) and inertia (*M*) coefficients are ~ isotropic, i.e., C_{XX}~C_{YY} and M_{XX}~M_{YY}. Cross-coupled coefficients are small for most whirl type motions.

(b) Simple theory does a modest job in producing physically accurate results for test SFDs with feed groove.

(c) SFDs generate large added mass coefficients, more so for sealed ends configurations and with (deep) feed and discharge grooves.

Conclusion (2):

(d) A sealed SFD produces significantly (3+X) more damping and ~twice the added mass than an open ends SFD.

(e) The amplitude and shape of whirl motion have small effect on the SFD force coefficients.

(f) Air ingestion impairs the growth of film pressures for increasing orbit amplitudes and frequency → damping coefficients decrease.

The experimental results demonstrate SFDs are mostly linear mechanical elements.

Integral SFDs

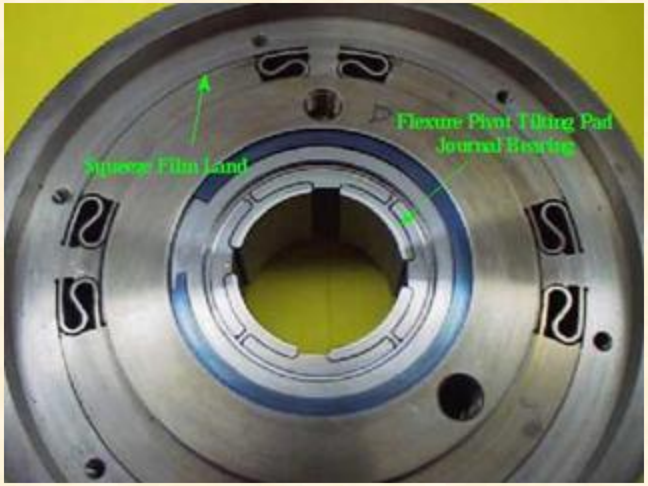

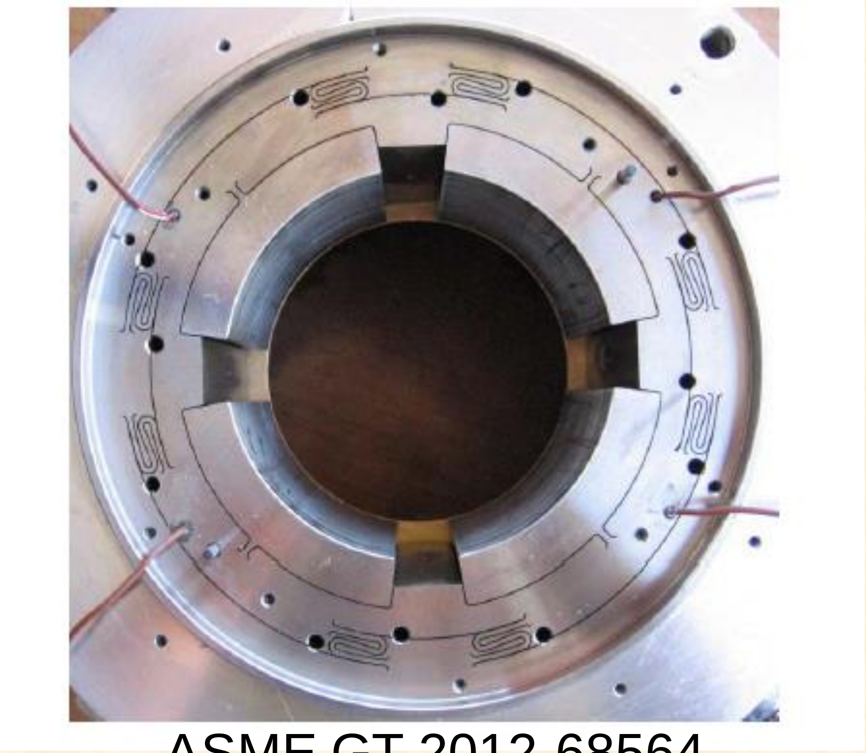

ASME GT 2012-68564

A few pointers …

Integral Squeeze Film Damper (ISFD)

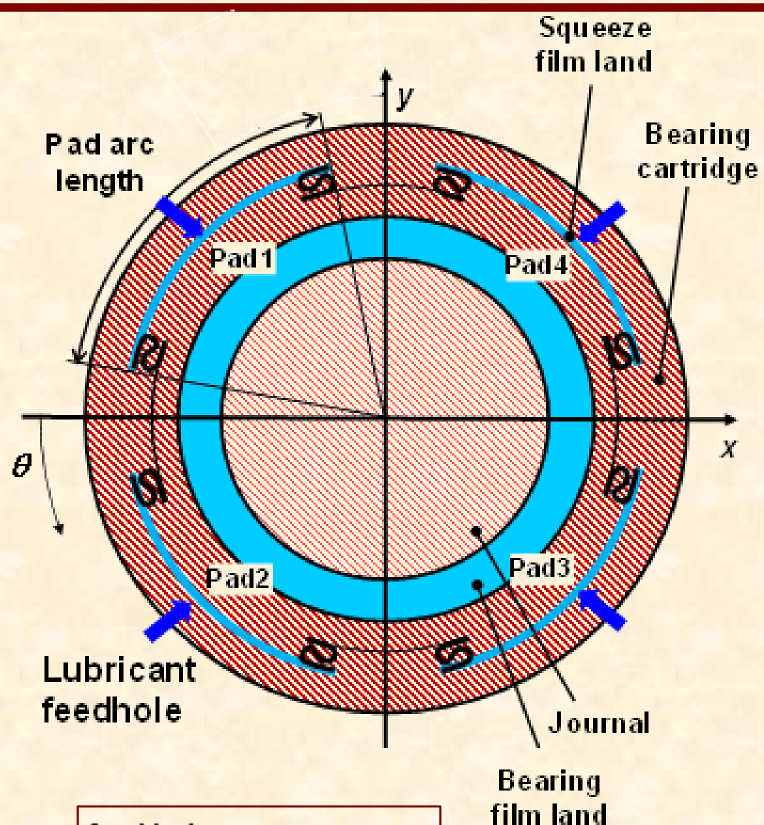

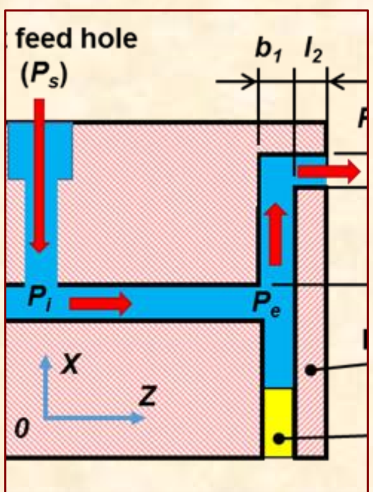

No squirrel cage

EDM manufacturing process produces separate arcuate damper film lands with S-shape flexural springs.

Advantages

- **low number of parts**
- **short axial span**
- **light weight**
- **higher tolerance precision.**

ISFDs: the sum of experiments

2011 **Identification of Force Coefficients in a 5-pad Tilting Pad Bearing with an Integral Squeeze Film Damper** **(Delgado et al. at GE)**

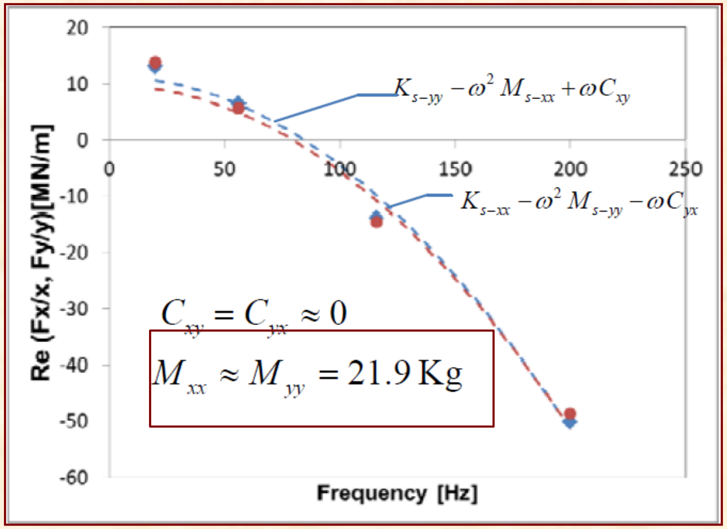

GT2012-68564 **Rotordynamic Characteristics of a Flexure Pivot Pad Bearing with an Active and Locked Integral Squeeze Film Damper** **(Agnew and Childs)**

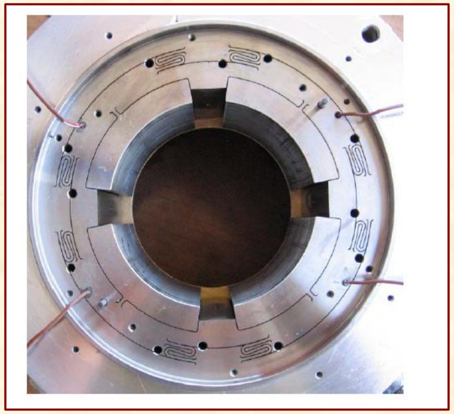

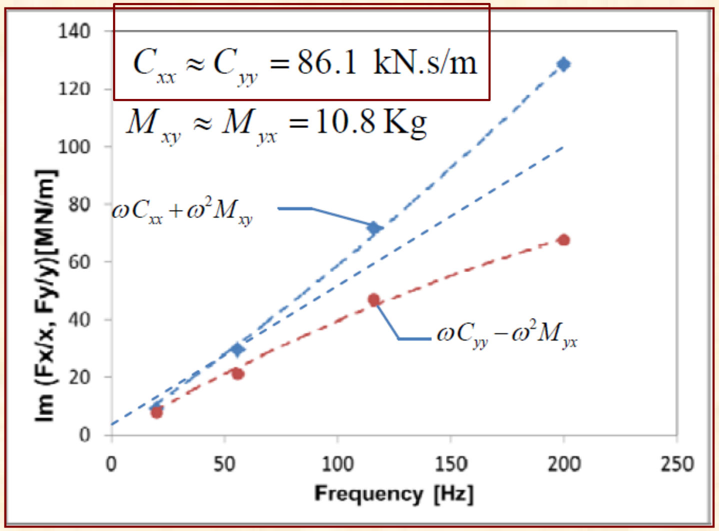

2017 **Dynamic Characterization of an Integral Squeeze Film Bearing Support Damper for a Supercritical CO_2 Expander** **(Ertas et al. at GE)**

ISFD produces significant damping & inertia coefficients.

ISFD tests in Delgado (2011)

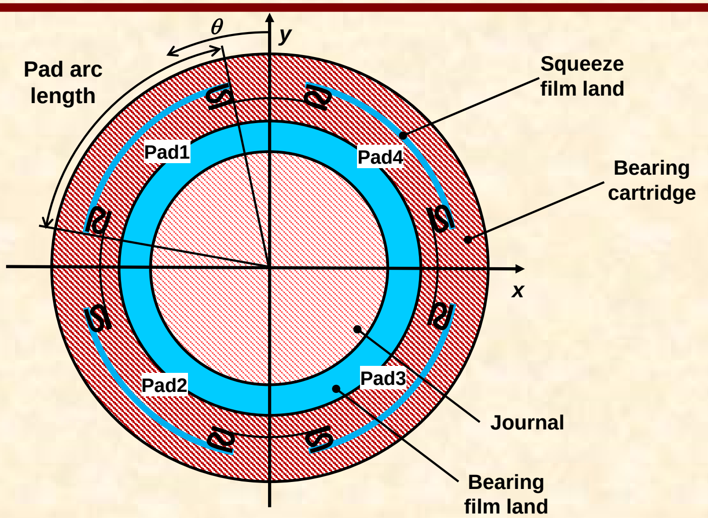

Parameter	Magnitude
Clearance	0.58 mm
Diameter	169 mm
Length	44 mm
Number of segments	4
Segment arc	60 °

Model predicts well damping but over-estimates inertia by 30%.

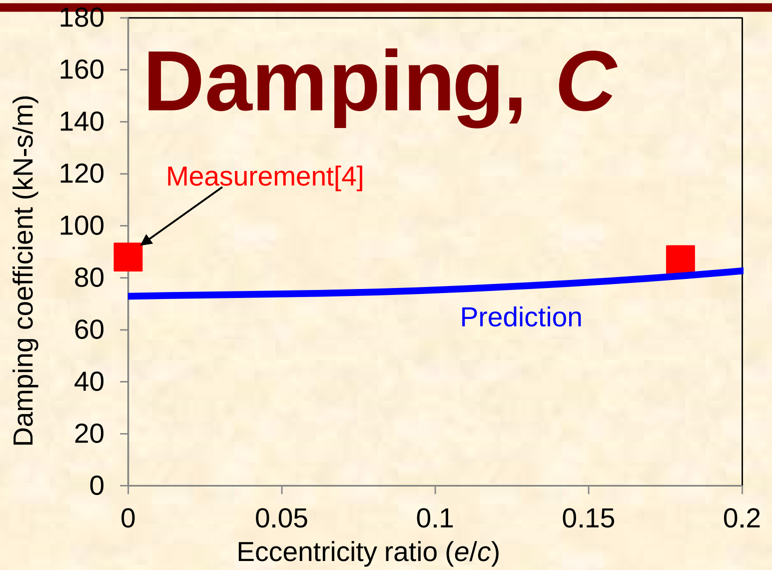

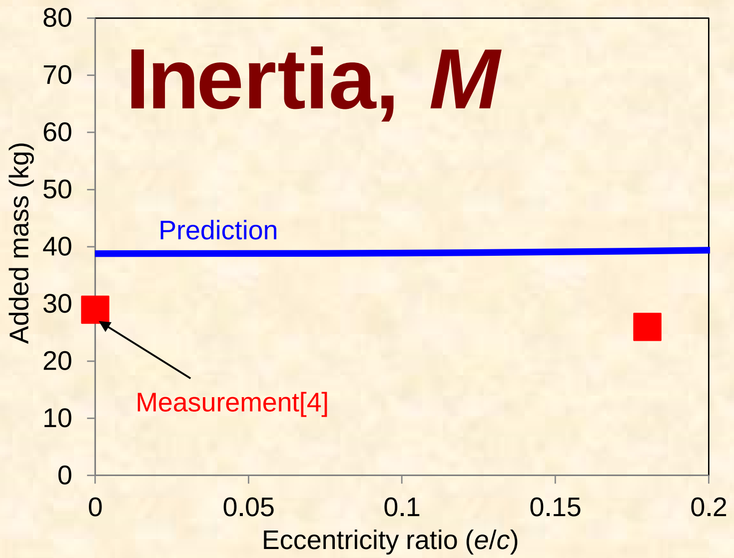

Our aim

End seals amplify viscous damping!

Quantify the effect of various end seal gaps on the dynamic forced performance of an ISFD.

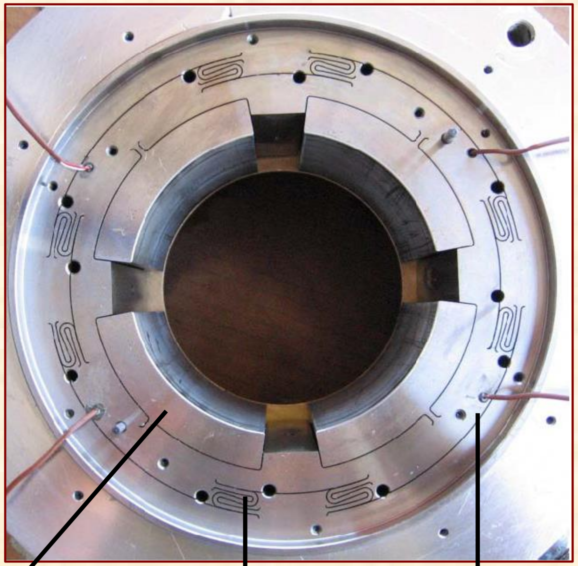

- **2019: Conduct dynamic load tests on a dedicated test rig to obtain ISFD force coefficients for ready comparison and validation of the model.**

Test ISFD → Load between pads

ISFD inner ring

ISFD outer ring

Bearing Cartridge (BC)

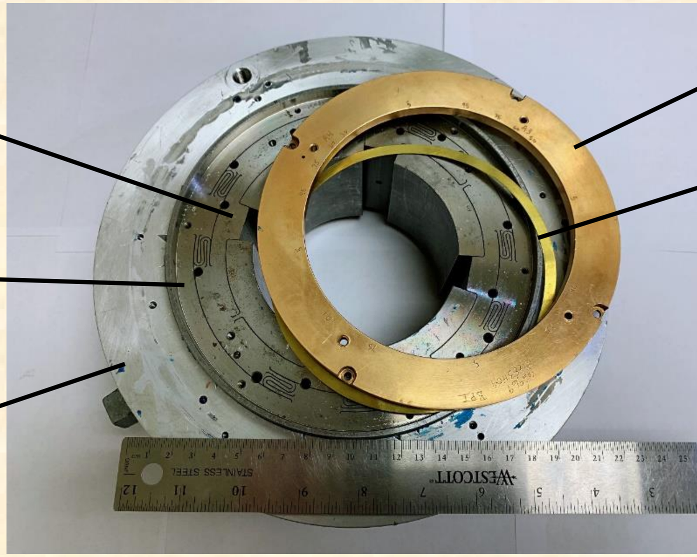

End plate

Shim

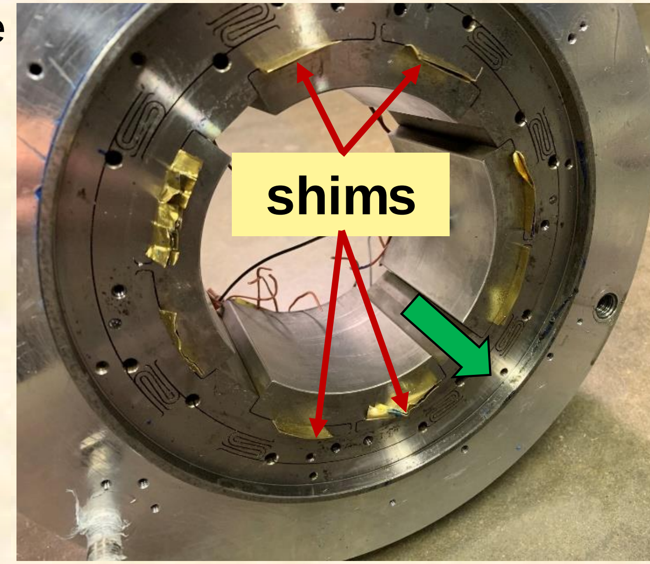

Diameter at film land, D_{ISFD}	**157 mm (6.18 in)**
Length, L	**76 mm (3 in)**
Film clearance, c	**0.356 mm (14 mil)**
Arc radius, α	**73° - 4 pads**
End seals gap, b_1	**0.28 mm, 0.43 mm, 0.53 mm, open ends**
ISO VG46 Viscosity, μ	**31.2 cP (at 46 ºC)**
Density, ρ	**860 kg/m^3**
Supply flow rate, Q	**9.5 L/min (set pressure)**

End seals ISFD → Shimmed End Plates

$$\frac{l_1}{b_1^3} > \frac{l_2}{b_2^3}$$

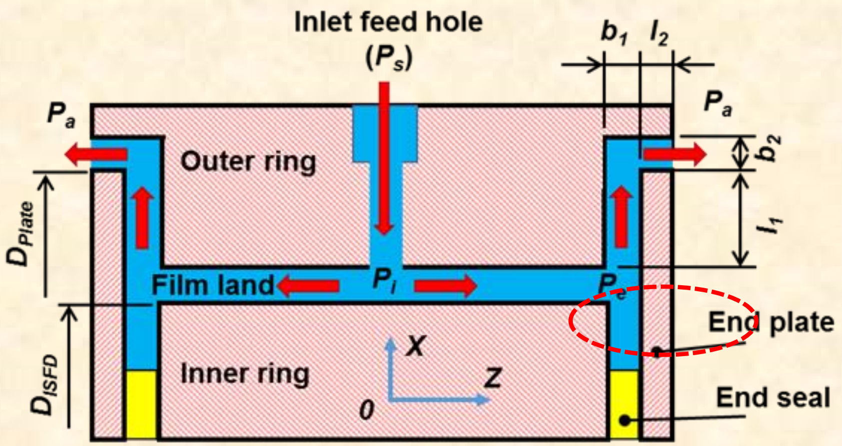

l_1 = 7.75 mm, l_2 = 6.35 mm,
b_2 = 0.85 mm >> b_1
D_{ISFD}=157 mm,
D_{plate}=172.5 mm.

ISFD film clearance
***c*=0.356 mm (14 mil)**

End seals gap = shim thickness b_1

b_1 (mm)	c/b_1
0.53	1.49
0.43	1.21
0.28	0.79

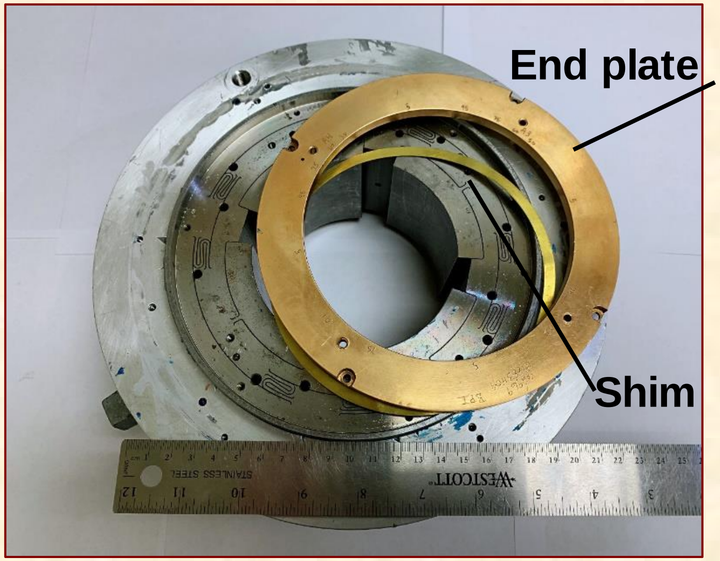

Test Rig for Dynamic Load Experiments

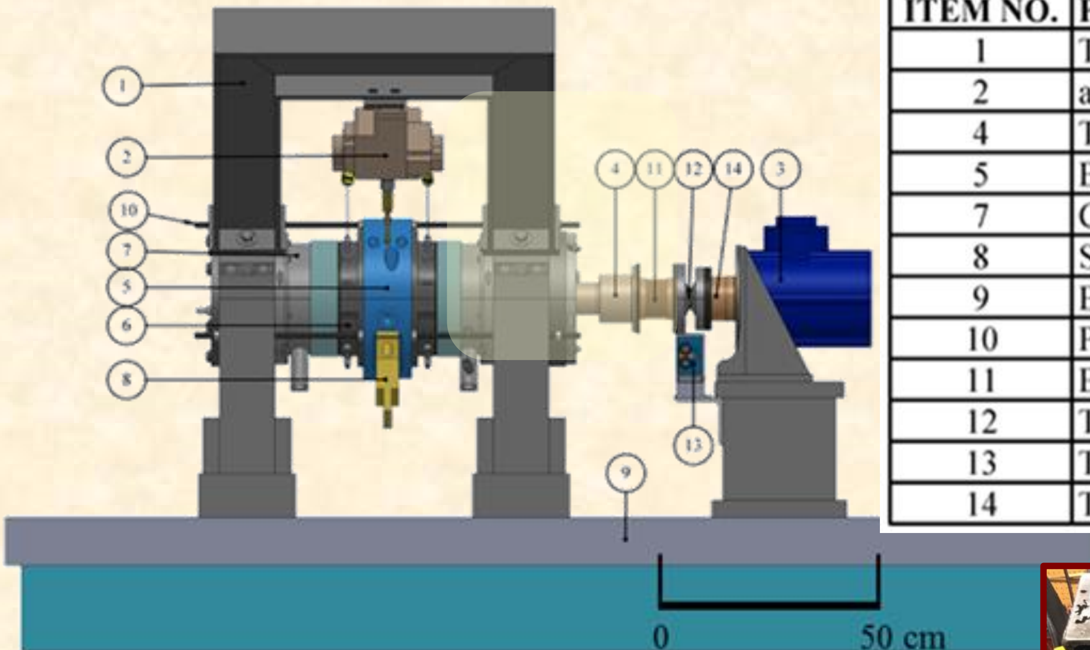

ITEM NO.	PART NO.
1	Test-rig pedestals
2	air turbine motor
4	Test rotor
5	Bearing stator
7	Collection Chambers
8	Static Loader Yoke
9	BedPlate
10	Pitch stabilizer bolts
11	Bellow Coupling
12	Torque meter (rotor)
13	Torque meter (stator)
14	Torque limiter

Max Speed:16 krpm

Max Static Load: 22 kN

Max Dynamic Load:

4.4 kN, 1 k Hz

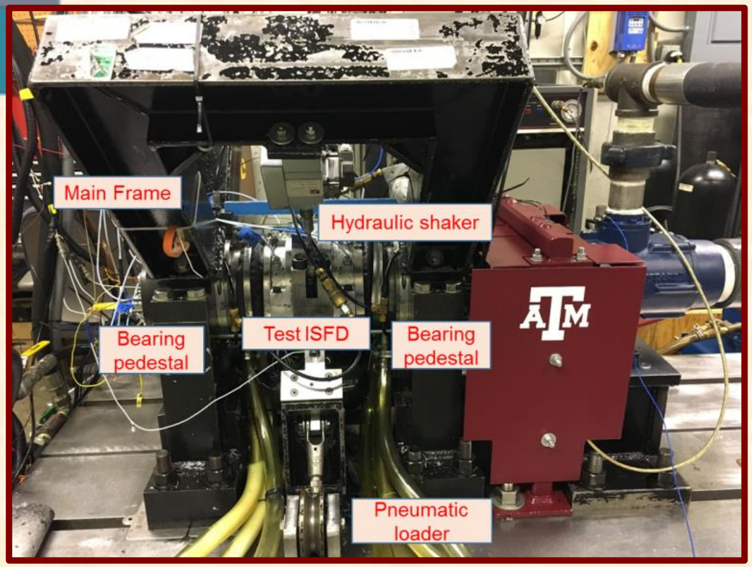

ISFD (lubricated) dynamic complex stiffness H_L

$(K, C, M)_{SFD} = (K, C, M)_L - (K, C, M)_S$

SFD Film — Test system (Lubricated) — Dry structure

Centered *e*=0.
Open ends and with end seals
gap = 0.53 mm → 0.28mm

$\mathrm{Re}(\mathbf{H}_L) \rightarrow (\mathbf{K}_L - \omega^2 \mathbf{M}_L)$

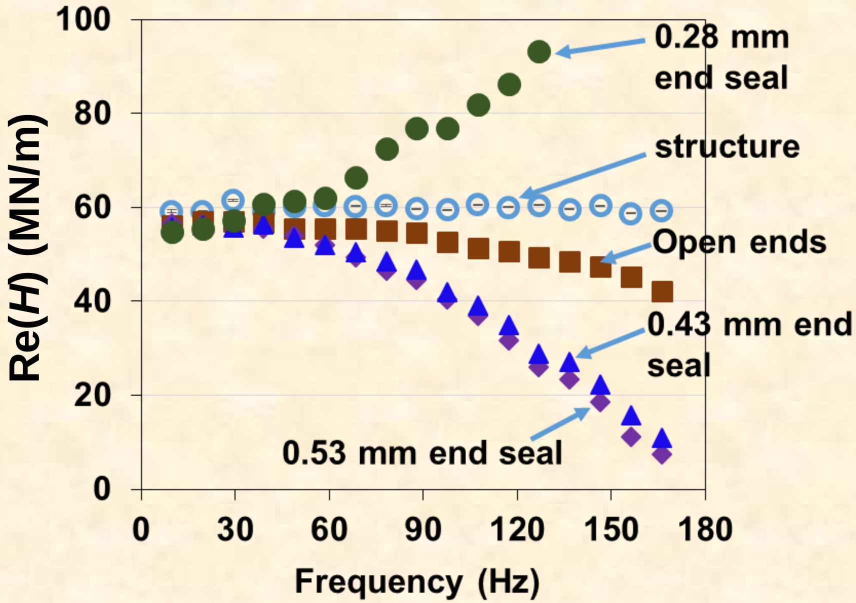

$\mathrm{Im}(\mathbf{H}_L) \rightarrow (\mathbf{C}_L \omega)$

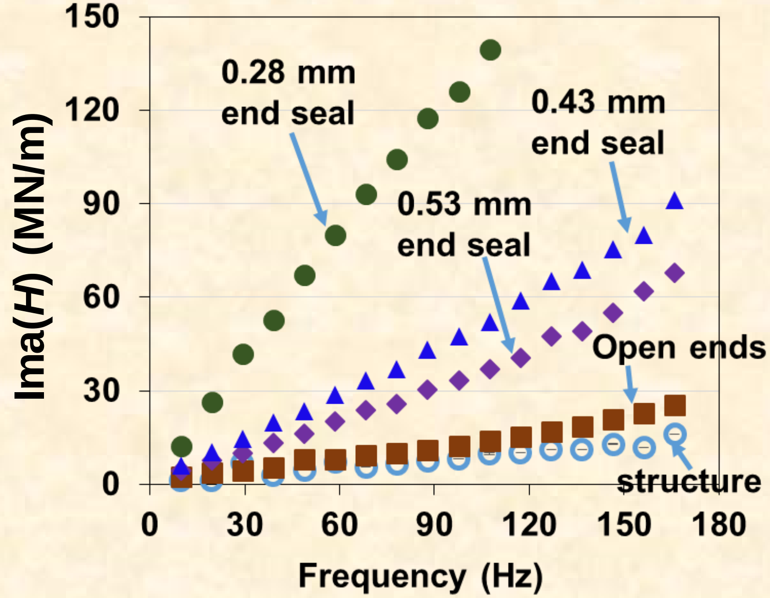

Structure — Open ends — 0.53 mm end seal — 0.43 mm end seal — 0.28 mm end seal

Stiffness vs. static eccentricity vs. gap in end seal

GT2020-14182

$K = \frac{1}{2}\,(K_{XX}+K_{YY})$ [MN/m]

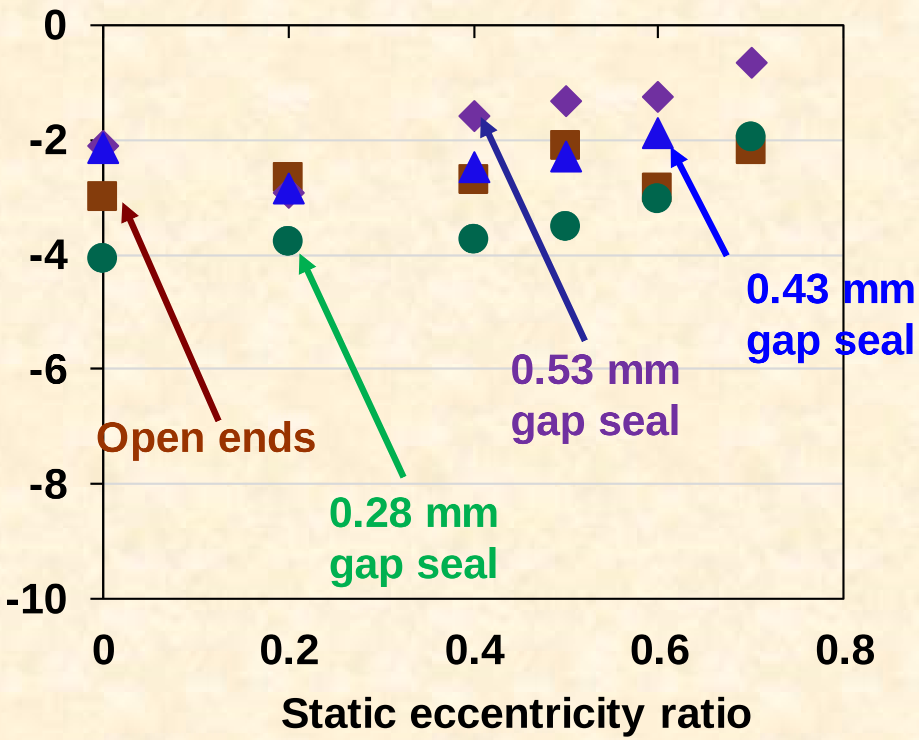

ISFD film stiffness *K* is small.

S-structure stiffness ~ 60 MN/m)

Open ends | 0.53 mm end seal | 0.43 mm end seal | 0.28 mm end seal

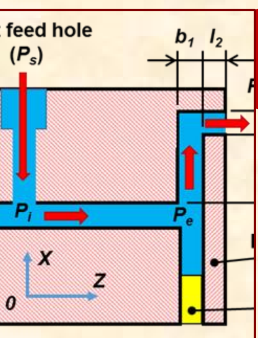

c=356 μm, e/c=0-0.7, ω=9-166 Hz, Q~9.5 L/min, P_s=1 ~ 2 barg

Damping vs. static eccentricity vs. gap in end seal

GT2020-14182

(C_{XX}, C_{YY}) [kN.s/m]

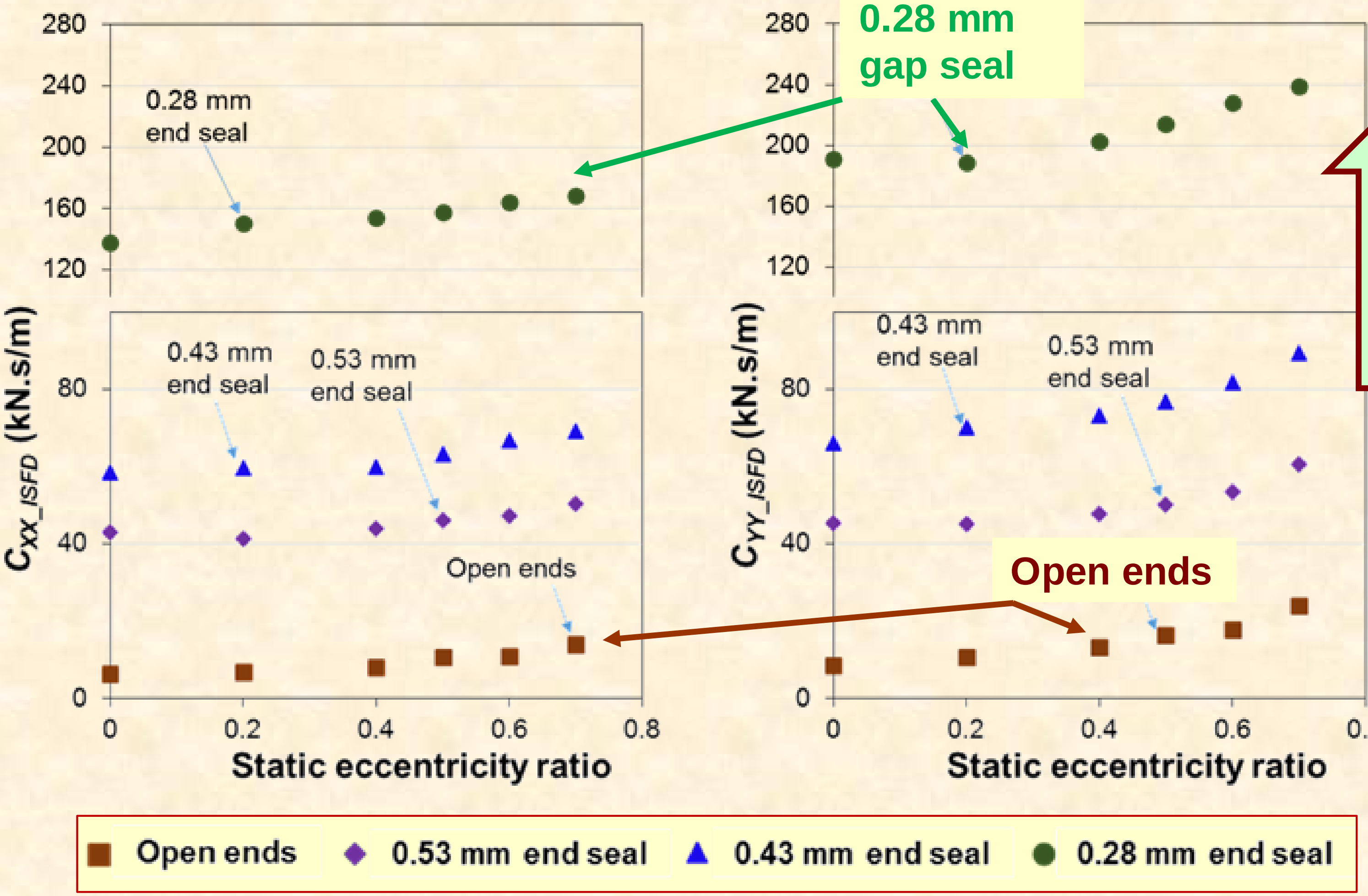

Damping increases 22 times from open ends → ends seal with gap = 0.28mm

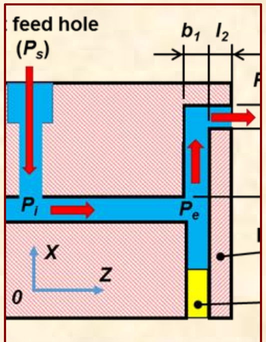

***c*=356 μm, *e/c*=0-0.7, 9-166 Hz, *Q*~9.5 L/min, P_s=1 ~ 2 barg**

Added mass vs. static eccentricity vs. gap in seal

(M_{XX}, M_{YY}) [kg]

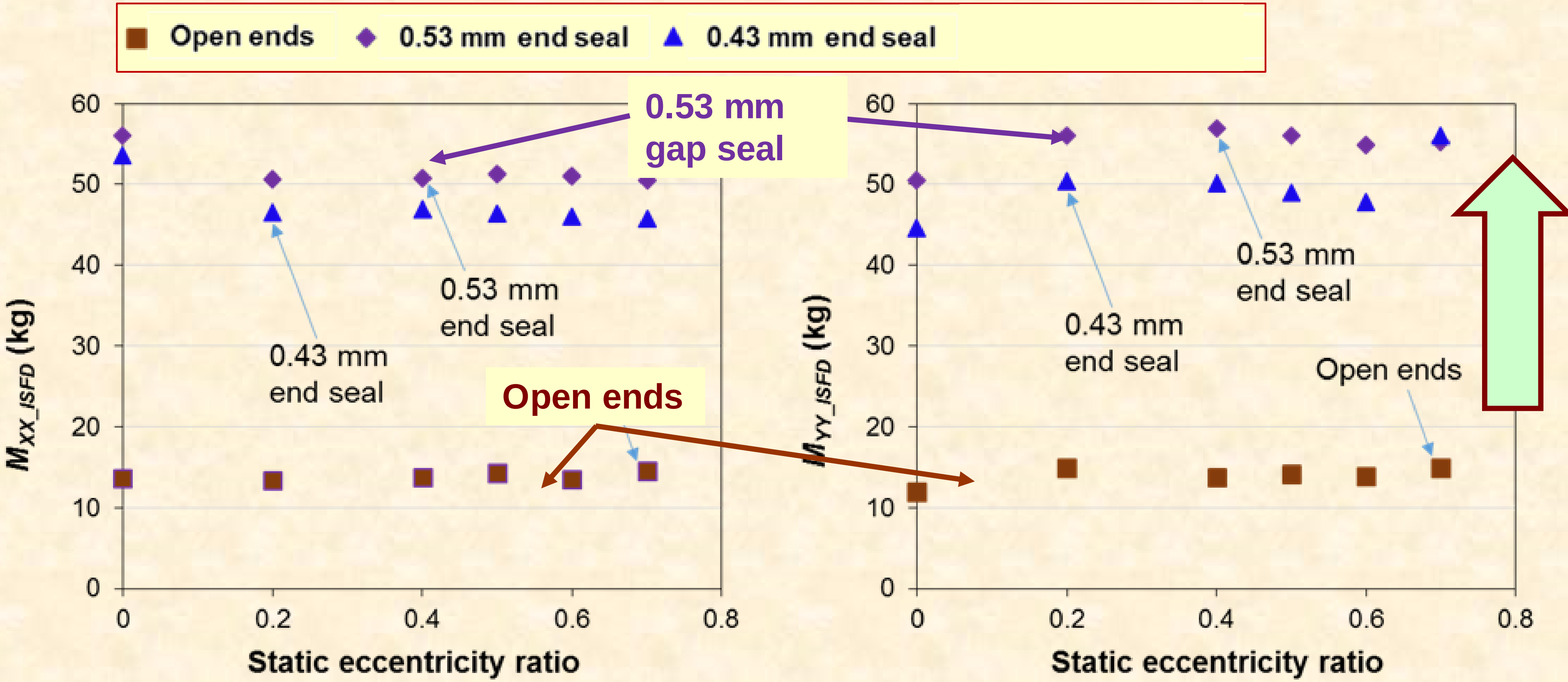

Inertia coefficient (added mass) larger than bearing mass (19 kg)

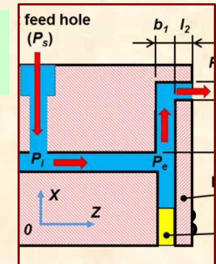

c=356 μm, *e*/*c*=0-0.7, 9-166 Hz, *Q*~9.5 L/min, P_s=1 ~ 2 barg

Conclusion ISFDs

(a) ISFD does not produce a film direct stiffness K_{ISFD} except for the test condition with the tightest end seal.

(b) Damping C_{ISFD} increases with static eccentricity (large static load) but not as pronounced as theory predicts.

(c) Added mass M_{ISFD} increases as gap decreases but ISFD with tightest gap (b_1 = 0.28 mm < c) produces a stiffening hardening (negative virtual mass).

(d) End seals with small gap amplify C_{ISFD}. Configuration with gap b_1=0.28 mm produces 22 more damping that the open ends ISFD.

(e) For static eccentricity (e<0.4c), model with fluid compressibility predicts well the ISFD experimental damping coefficients but not its added mass.

Acknowledgments

Thanks to

Pratt & Whitney Engines (2008-2018)

TAMU Turbomachinery Research Consortium (TRC)

Learn more:

http://rotorlab.tamu.edu

References

Relevant past work

- **Della Pietra and Adilleta, 2002, The Squeeze Film Damper over Four Decades of Investigations. Part I: Characteristics and Operating Features, Shock Vib. Dig, (2002), 34(1), pp. 3-26, Part II: Rotordynamic Analyses with Rigid and Flexible Rotors, Shock Vib. Dig., (2002), 34(2), pp. 97-126.**

- **Zeidan, F., L. San Andrés, and J. Vance, 1996, "Design and Application of Squeeze Film Dampers in Rotating Machinery," Proceedings of the 25th Turbomachinery Symposium, Turbomachinery Laboratory, Texas A&M University, September, pp. 169-188.**

- **Zeidan, F., 1995, "Application of Squeeze Film Dampers", Turbomachinery International, Vol. 11, September/October, pp. 50-53.**

- **Vance, J., 1988, "Rotordynamics of Turbomachinery," John Wiley and Sons, New York**

Parameter identification:

- **Tiwari, R., Lees, A.W., Friswell, M.I. 2004. "Identification of Dynamic Bearing Parameters: A Review," *The Shock and Vibration Digest*, 36, pp. 99-124.**

References SFDs

2018 San Andrés, L., Koo, B., and Jeung, S-H, **"**Experimental Force Coefficients for Two Sealed Ends Squeeze Film Dampers(Piston Rings and O-rings): An Assessment of Their Similarities and Differences, **ASME GT2018-76224**:

2017 San Andrés, L., **Den, S.,** and **Jeung, S-H**., 2018, "On the Force Coefficients of a Flooded, Open Ends Squeeze Film Damper: from Theory to Practice (and Back)," ASME J. Eng. Gas Turbines Power, Vol. **140**(1)**,** (ASME GT2017-63152)

2016 San Andrés, L., and Jeung, S.-H, 2016, Response of a Squeeze Film Damper-Elastic Structure System to Multiple Consecutive Impact Loads," ASME J. Eng. Gas Turbines Power. Vol. **138** (12), (ASME GT2016-56695)

2016 San Andrés, L., S-H Jeung, S. Den, and G. Savela, "Squeeze Film Dampers: A Further Experimental Appraisal of Their Dynamic Performance," Proceedings of the 45th Turbomachinery Symposium, Houston, TX, Sept 12-15. (Tutorial).

2015 San Andrés, L., Jeung, S-H, and Bradley, G., "Force Coefficients for a Short Length Open-Ends Squeeze Film Damper with End Grooves: Experiments and Predictions," ASME GT 2015-43096

2014 San Andrés, L., Jeung, S-H, and Bradley, G., "Experimental performance of a Open Ends Centrally Grooved Squeeze film Damper Operating with Large Amplitude Orbital Motions," ASME GT 2014-25413.

2014 San Andrés, L., "Force Coefficients for a Large Clearance Open Ends Squeeze Film Damper with a Central Groove: Experiments and Predictions," Tribol. Int., **71**, pp. 17-25

2013 San Andrés, L., and Seshagiri, S., "Damping and Inertia Coefficients for Two End Sealed Squeeze Film Dampers with a Central Groove: Measurements and Predictions," ASME J. Eng. Gas Turbines Power, **135**(12), p. 112503.

2012 San Andrés, L., 2012, "Damping and Inertia Coefficients for Two Open Ends Squeeze Film Dampers with a Central Groove: Measurements and Predictions," ASME J. Eng. Gas Turbines Power, 134(10), p. 102506.

2012 San Andrés, L., and Delgado, A., "A Novel Bulk-Flow Model for Improved Predictions of Force Coefficients in Grooved Oil Seals Operating Eccentrically," ASME J. Eng. Gas Turbines Power, 134(5), p. 052509.

References SFDs

2010	Delgado, A., and San Andrés, L., 2010, "A Model for Improved Prediction of Force Coefficients in Grooved Squeeze Film Dampers and Grooved Oil Seal Rings", ASME J. Tribol., 132(3), p. 032202.
2012	San Andrés, L., 2012, "Squeeze Film Damper: Operation, Models and Technical Issues," Modern Lubrication Theory, Notes 13, Texas A&M University Digital Libraries, https://repository.tamu.edu/handle/1969.1/93197
2010	Delgado, D., and San Andrés, L., 2010, "Identification of Squeeze Film Damper Force Coefficients from Multiple-Frequency, Non-Circular Journal Motions," ASME J. Eng. Gas Turbines Power, Vol. 132 (April), p. 042501 (ASME Paper No. GT2009-59175)
2009	Delgado, A., and San Andrés, L., 2009, "Nonlinear Identification of Mechanical Parameters on a Squeeze Film Damper with Integral Mechanical Seal," ASME Journal of Engineering for Gas Turbines and Power, Vol. 131 (4), pp. 042504 (ASME Paper GT2008-50528)
2003	San Andrés, L., and S. Diaz, 2003, "Flow Visualization and Forces from a Squeeze Film Damper with Natural Air Entrainment," ASME Journal of Tribology, Vol. 125, 2, pp. 325-333
2001	Diaz, S., and L. San Andrés, 2001, "Air Entrainment Versus Lubricant Vaporization in Squeeze Film Dampers: An Experimental Assessment of their Fundamental Differences," ASME Journal of Gas Turbines and Power, Vol. 123 (4), pp. 871-877
2000	Tao, L., S. Diaz, L. San Andrés, and K.R. Rajagopal, 2000, "Analysis of Squeeze Film Dampers Operating with Bubbly Lubricants" ASME Journal of Tribology, Vol. 122, 1, pp. 205-210
1997	Arauz, G., and L. San Andrés, 1997 "Experimental Force Response of a Grooved Squeeze Film Damper," Tribology International, Vol. 30, 1, pp. 77-86
1996	San Andrés, L., 1996, "Theoretical and Experimental Comparisons for Damping Coefficients of a Short Length Open-End Squeeze Film Damper," ASME Journal of Engineering for Gas Turbines and Power, Vol. 118, 4, pp. 810-815